CYTOTOXIC ACTIVITY OF DESIGNED PEPTIDES BASED ON THE HUMAN ERYTHROPOIETIN SEQUENCE

by

Cynthia S. Quan

A thesis submitted in conformity with the requirements
for the degree of Master of Science
Graduate Department of Medical Biophysics
University of Toronto

Cytotoxic Activity of Designed Peptides based on the Human Erythropoietin Sequence

Cynthia S. Quan

Master of Science 2000

Graduate Department of Medical Biophysics

University of Toronto

Abstract

In this study, we set out to develop a general method for designing antagonists of helical cytokines. Our method involved grafting short amphipathic segments of a helical cytokine, which contained biologically important residues, onto a helical scaffold to produce a 3-helix bundle with molten globule structure. Erythropoietin (EPO) was used as a model cytokine. Six potential antagonist peptides were designed, synthesized and found to possess the expected helical and molten globular characteristics. However, they lacked specific antagonist activity and did not bind the soluble EPO receptor (EPOR). The designed peptides showed an unexpected cytotoxicity which appeared to be acting through necrosis. Surprisingly, the regions of EPO grafted onto the scaffold, which confer cytotoxicity, correspond to the EPOR-binding sites of EPO. Therefore, it appears that the sequence encoding the receptor-binding sites of EPO also encodes cytotoxic activity when isolated and presented in a helical conformation.

Acknowledgements

Many people have shared in the ups and downs, joyful and unbearable times of my M.Sc. journey. This thesis would be incomplete without acknowledging them.

I am indebted to my supervisor, Avi Chakrabartty, who gave me the freedom to pursue independent scientific research, while at the same time provided the required support and guidance. I am grateful for the many times I've benefited from your ability to teach and explain difficult scientific concepts (sometimes more than once! ☺). Thanks for always being the voice of optimism, and for believing in my ability to see this project to the end. I also extend my appreciation to Dwayne Barber, for his expertise on the 'cell'-side of my work and to Chris Richardson and Cheryl Arrowsmith for their constructive comments.

To the Chakrabartty lab (Chandra, Sandy, Paul, Jackson and Qi), thanks for showing me the ropes in the protein folding field. You guys made work an entertaining place to be! ☺ Special thanks to Chandra for her encouragement and help in editing 'the monster'!

To the Barber lab (Bryan, Jackie, Adrienne, Melody, and Jenny), thanks for accepting me as an 'appendage' to your lab and for all your technical advice. Special thanks to Melody for her 'expertise' in FACS – without you, I might be still working on my 'last experiment'!

To Connie, thanks for taking the first few steps of grad school with me and for your enthusiasm for scientific research.

To Wai-May, thanks for the laughs while you were still at PMH...you taught me that people are more important than the tasks that we are doing – thanks.

Clare, our faith-talks have always been inspiring – they have added a new dimension to lab work! Thanks for the talks on the "real important" things in life and for sharing in life's joy and struggles.

Peter O'Dwyer – you once said, "I'll hire you with the assumption that you'll get your PhD one day" -wow! Thanks for the vote of confidence – this played a significant role in my decision to pursue grad studies.

To Rebecca and Anita, thanks for your faithful friendship and walking the daily grind with me!

To my ETCBC family – thanks for all your prayers and coping with me in stress-mode! Special thanks to...

Norm – what can I say, it's like you did another thesis eh? Thanks for EVERYTHING: sharing your Master's wisdom, lending a listening ear...and for the many hours of thesis editing! ☺

Alfred – to one of the most encouraging people I know, thanks for all your grad school wisdom...you have been a dear friend through the ups and downs of the thesis and life! and to Ms. Anna – thanks for all the 'behind the scene' support ☺

Jason – thanks for the time you spent helping me study, and for being a calm voice in some of the crazier moments of presentations and thesis writing.

Daniel Fellowship – you guys have been great! Thanks for all your smiles and prayers.

To Anna Yuen – the only person who offered to read my thesis 2x on her own accord, crazy girl! thanks!!

A huge thanks to my family: mom, dad and Timmy, for your love and support (thanks for the many tofu containers of food mom!)

...all to and for the glory of God!

Table of Contents

List of Tables

List of Figures

Abbreviations

EPO	erythropoietin
EPOR	erythropoietin receptor
rhEPO	recombinant human erythropoietin
HIF-1	hypoxia-induced factor-1
HNF-4	hepatic nuclear factor-4
IL	interleukin
JAK	Janus kinase
SH2	Src homology 2
STAT	signal transducers and activators of transcription
MAPK	Mitogen-activated protein kinase
PI3-kinase	phosphatidylinositol 3-kinase
EPObp	extracellular ligand-binding domain of the EPOR (complexes with EPO)
EBP	extracellular ligand-binding domain of human EPOR (complexes with non-native ligands)
FBN	fibronectin
EMP	EPO mimetic peptides
PEG	polyethylene glycol
IgG	immunoglobulin G
DHFR	dihydrofolate reductase
GH	growth hormone

PRL	prolactin
G-CSF	granulocyte-colony-stimulating factor
GM-CSF	granulocyte-macrophage colony-stimulating factor
TPO	thrombopoietin
LIF	leukemia inhibitory factor
SCF	stem cell factor
CNTF	ciliary neurotrophic factor
CRH	cytokine receptor homology
Fmoc	fluorenylmethoxycarbonyl
XTT	sodium 3,3'-{1-[(phenylamino)carbonyl]-3,4-tetrazolium}-bis(4-methoxy-6-nitro)benzene sulfonic acid hydrate
7-AAD	7-amino-actinomycin D
bZIP	basic region leucine zipper

Chapter 1: Introduction

The study of cytokines is extremely important because they play a critical role in numerous physiological processes such as red blood cell production and the immune defence. Abnormal cytokine production is implicated in various diseases, ranging from rheumatoid arthritis to cancers, making them a target for drug design. In fact, helical cytokines such as erythropoietin (EPO), growth hormone and alpha-interferon, have been successfully developed as drugs. However, their lack of desirable pharmacological properties such as oral and topical delivery has severely limited their entry into the pharmaceutical markets. Thus, designing small molecule agonists and antagonists of helical cytokines would serve as an intermediate step towards drug design. Construction of peptides and proteins with the desired structure and biological function is now becoming a feasible goal as more information is being discovered about how an amino acid sequence determines a protein's three-dimensional structure and how this structure confers the biological function.

In the present study, we have set out to design antagonists of helical cytokines. The fundamental requirement for structure-based design of antagonists to a helical cytokine receptor is understanding the factors that contribute to the molecular recognition process. EPO was chosen as a model cytokine to test our design strategy because of the wealth of available structural and biological data on EPO and the similarities in structure between EPO and other helical cytokines. This chapter will provide an overview of the basic biology of EPO, identify the structural and functional sites of EPO needed for binding to the EPO receptor (EPOR), review the recent structural studies that have given new insight into EPOR activation and highlight the structural similarities of EPO and other helical cytokines.

A. A Brief Overview of EPO Biology

Erythropoietin (EPO) is a 34 kDa glycoprotein composed of 165 amino acids and has a carbohydrate content of 39% (Davis et al., 1987). EPO is the primary hormone that regulates mammalian erythropoiesis (Erslev, 1953; Miyake et al, 1977). This process involves the survival, proliferation and terminal differentiation of erythroid precursors, resulting in an increase of red blood cell production. In 1977, EPO was purified from the urine of aplastic anemia patients (Miyake et al., 1977) and in 1985, a full length cDNA was isolated (Jacobs et al., 1985; Lin et al., 1985). In the following year, recombinant human EPO (rhEPO) was produced in mammalian cells and found to be biologically active and equivalent to the natural hormone (Egrie et al., 1986). Today, rhEPO is used worldwide for the treatment of anemias associated with renal failure, chemotherapy and AIDS (Ebert and Bunn, 1999).

I. Production and Regulation of EPO

In mammals, EPO is primarily produced in fetal liver (Zanjani et al., 1977) and adult kidney (Koury et al., 1988; Lacombe et al., 1988) in response to hypoxia. However, low levels of EPO mRNA have been detected in kidneys and livers of unstimulated mice and rats suggesting a low basal level of EPO in the serum (Fandrey and Bunn, 1993). Regulation of EPO production is controlled at the mRNA level. A 50 base pair hypoxia-inducible enhancer has been identified at the 3' end of the gene and is responsible for hypoxia-induced EPO gene expression. This site is bound by transcription factors, hypoxia-induced factor-1 (HIF-1) and hepatic nuclear factor-4 (HNF-4) (McMillin and Percy, 1999). Interaction between these factors and the transcription activator p300 provides a mechanism for the induction of EPO

gene expression (McMillin and Percy, 1999). Although hypoxia is the main stimulus for production of EPO (Ebert and Bunn, 1999), transition metals and iron chelators such as cobalt (Goldberg et al., 1988) and desferrioxamines (Wang and Semenza, 1993), respectively, also cause a marked increase in the expression of EPO mRNA and the production of EPO.

II. EPO Receptor

EPO circulates in the bloodstream where it binds to EPO receptors (EPOR) on committed erythroid progenitor cells in the bone marrow (Ebert and Bunn, 1999). Other cells known to express EPOR include megakaryocytes, endothelial cells and possibly neurons (Lacombe and Mayeux, 1999). EPOR is a 66 kDa protein made up of 508 amino acids. It consists of an extracellular ligand-binding domain, a single transmembrane domain and a cytoplasmic domain (D'Andrea et al., 1989). EPOR belongs to the class I cytokine receptor superfamily which includes the receptors for growth hormone, prolactin, granulocyte- and granulocyte-macrophage colony-stimulating factors, thrombopoietin, leukemia inhibitory factor, interleukin (IL)-3, IL-4, IL-5, IL-6, IL-7, IL-9, IL-11, IL-12, IL-13, and IL-15 (Bazan, 1990; Wells and de Vos, 1996). Members of this family display two distinctive motifs in their extracellular ligand-binding domain: an amino-terminal set of four conserved cysteines that form two disulfide bonds and a WSXWS motif, where X represents any amino acid, near the transmembrane domain. The role of the WSXWS sequence appears to be in folding and transport of the receptor to the cell surface (Miura and Ihle, 1993). Although the class I cytokine receptor superfamily lacks intrinsic tyrosine kinase activity (Youssoufian et al., 1993), the cytoplasmic domain of EPOR contains a conserved β-chain

cytoplasmic box 1 motif, which binds specifically to the protein kinase Janus kinase 2 (JAK2), and eight phosphotyrosine sites that participate in downstream signal transduction (Wojchowski et al., 1999).

III. Intracellular events

Binding of EPO to cells expressing EPOR causes oligomerization of the receptors and induces autophosphorylation of the protein kinase JAK2. This kinase physically associates with a membrane-proximal region of each EPOR cytoplasmic domain (Witthuhn et al., 1993). Once activated, JAK2 phosphorylates Tyr residues on EPOR (Witthuhn et al., 1993), which serve as docking sites for intracellular signaling proteins with Src homology 2 (SH2) domains (Klingmüller et al., 1996). One such protein is STAT5, a member of the signal transducer and activator of transcription (STAT) family of transcription factors. EPO activates two isoforms of STAT5, STAT5a and STAT5b (Klingmüller et al., 1996). Upon phosphorylation, STAT5 either homodimerizes (STAT5a/STAT5a or STAT5b/STAT5b) or heterodimerizes (STAT5a/STAT5b), translocates to the nucleus and regulates the transcription of various genes (Klingmüller et al., 1996). The RAS-MAPK (Torti et al., 1992) and PI3-kinase (Damen et al., 1993) pathways are also activated.

IV. Mechanism of EPOR activation

It has been generally accepted that the activation of EPOR requires homodimerization of the receptor; more specifically, a single hormone binds to two receptor monomers forming a 2:1 receptor:ligand assembly (Wilson and Jollife, 1999). This stoichiometry requires two distinct surfaces on the ligand to contact the binding regions of two receptor monomers.

Matthews et al. (1996) has proposed a sequential dimerization mechanism for EPOR activation. Essentially, the two surfaces on EPO were identified as two distinct receptor-binding sites. The first receptor-binding site on EPO binds one receptor molecule with a certain affinity constant K_1. A second receptor molecule binds the 1:1 EPO:EPOR complex on the cell surface with an affinity constant K_2, where $K_2 > K_1$, and forms a complex of one EPO molecule bound to two identical receptors. However, the hypothesis that simple dimerization is sufficient for activation has been challenged by recent structural studies of EPOR binding with multiple non-native ligands (Livnah et al., 1996; Livnah et al., 1998; Livnah et al., 1999). Although all of these ligands were able to homodimerize EPOR, activation was only observed in a subset of these molecules. This has led to new insights for EPOR activation involving specific orientations of the receptor. These studies will be reviewed in the latter part of this chapter.

B. Structure-Function Relationship of EPO

I. Structure Determination of EPO

In the early 1990s, the structure of EPO had yet to be solved by X-ray diffraction or NMR. To gain an understanding of the structure-function relationship, Boissel et al. (1993) generated a computer model of EPO based on the primary sequence of EPO and the location of its disulfide bonds. It was suggested that EPO was made up of α-helices in a 4-helix bundle. Initial attempts at determining the crystal structure of EPO using the unglycosylated, bacterially expressed form of EPO were unsuccessful due to the limited solubility and stability of the protein in the absence of its carbohydrate chain. To circumvent these

problems, an EPO analogue was made with the N-linked glycosylation sites mutated to Lys residues and a Met and Lys residue added to the N-terminus for higher expression yields in *E. coli.* This mutant (MKLysEPO) showed increased solubility and was used in NMR studies (Cheetham et al., 1998). Similar challenges were experienced in attempting to grow crystals of EPO complexed to the extracellular ligand-binding domain of the EPOR (EPObp) for X-ray diffraction studies. Eventually a variant of MKLysEPO, with two additional mutations, P121N and P122S, was used. The EPObp was expressed in *Pichia pastoris* cells, with the N-linked glycosylation removed by an N52Q mutation and an A211E mutation for better expression in cells (Syed et al., 1998). The crystal and solution structures of EPO were simultaneously solved in 1998 (Syed et al., 1998; Cheetham et al., 1998).

Both methods of structure determination reveal that EPO is a left-handed 4-helix bundle, with anti-parallel α-helices (A, B, C and D) in an up-up-down-down orientation (Fig. 1). These helices are connected by two long crossover loops (AB and CD) and a short loop (BC) of five residues linking Helix B and C together. This structure confirms the computer model of EPO generated by Boissel et al. (1993). The structural studies show that the N and C termini are linked together by a disulfide bond formed between Cys7 (Helix A) and Cys161 (Helix D). A second disulfide bond is located within the AB loop (Cys29-Cys33). Helix D contains a kink near the middle of its helix caused by a Gly residue at position 151. A short α-helical segment (B') is found near the carboxy end of the AB loop where it was previously predicted to be a β-sheet (Boissel et al., 1993) (Fig.1). In addition, an anti-parallel β-sheet is formed from the interactions of the long AB and CD crossover loops (β1- and β2-strands) (Fig. 1).

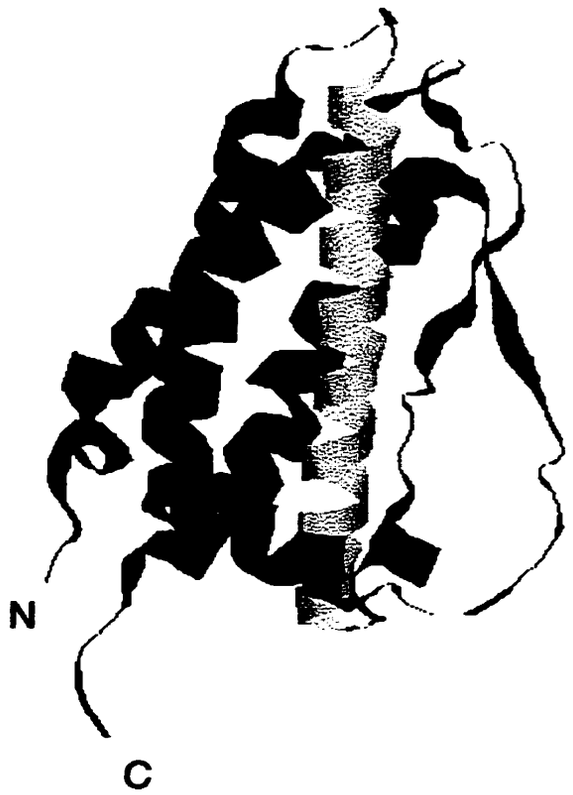

Fig. 1 X-ray Crystal Structure of Erythropoietin

The X-ray crystal structure of erythropoietin is shown as a ribbon diagram. The NH_2- and COOH-termini are marked N and C, respectively. The secondary structure elements are coloured as follows with the residues which make up the secondary structure element indicated in parentheses: red: Helix A(8-26)up; black: Helix B'(47-52); yellow: Helix B(55-83)up; purple: Helix C(90-112)down; light blue: Helix C'(114-122); green: Helix D(138-161)down; dark green: β1-strand(39-41); orange: β2-strand(133-135). Loops are coloured in blue. This diagram was generated from the PDB accession code 1EER using RASMOL.

Two differences are observed between the NMR and X-ray crystal structures. Although both the solution and crystal structures identify a small B' helix, this helix is displaced ~3 Å along the B:D helical interface of the protein in the crystal structure relative to the solution structure (Fig. 1). The crystal structure was solved as a complex of EPO bound to EPObp whereas the solution structure was solved with EPO alone. Therefore, the displacement observed in the crystal structure is likely due to EPO binding EPObp (Cheetham et al., 1998). The other difference observed is the presence of an additional short helix (C') at the start of the CD loop in the crystal structure which is not seen in the NMR structure (Fig. 1). This short helix is oriented 90° to the principal axis of Helix C (Cheetham et al., 1998). The solution structure shows this region to be highly flexible with an extended conformation.

The crystal structure of EPO bound to EPObp reveals that one molecule of EPO binds to two receptors (Fig. 2) (Syed et al., 1998). The structure of EPObp consists of a short N-terminal helix followed by two β-sandwich domains, D1 (N-terminal) and D2 (C-terminal), which are oriented ~90° to each other, linked by a short helical polypeptide linker. The D1 and D2 domains contain ~100 residues that fold into a β-sandwich consisting of seven anti-parallel β-strands characteristic of a fibronectin (FBN) type III fold. The N-terminal helix is located in a corner formed by the D1 and D2 domains and is close to the WSXWS motif in the D2 domain.

The EPO-$(EPObp)_2$ complex is held together by interactions involving two patches located on opposite sides of the EPO molecule (Fig. 2). These patches have been identified

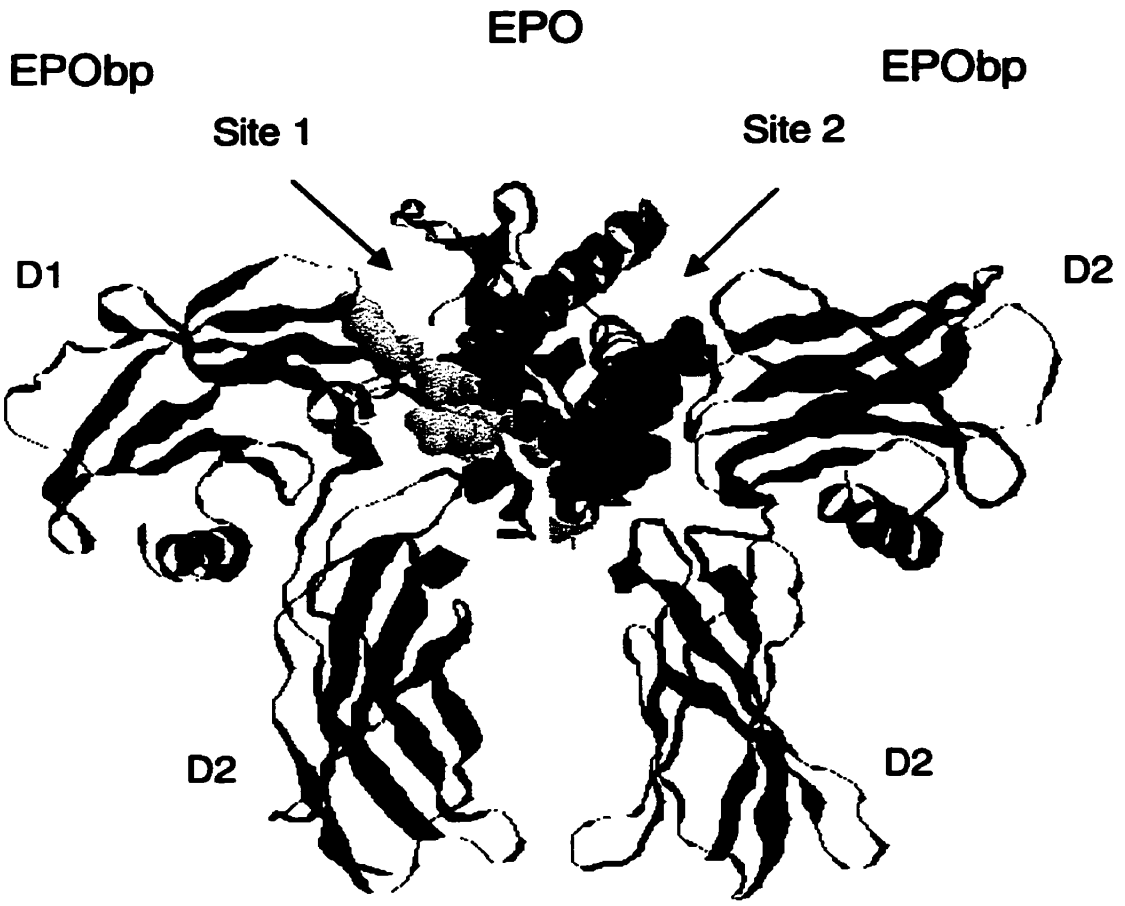

Fig. 2 Crystal Structure of EPO-(EPObp)$_2$

Ribbon diagram of the EPO-(EPObp)$_2$ complex. The two receptors (EPObp) are denoted in blue and green, and EPO is coloured in red. The two β-sandwich domains, D1 and D2, of EPObp are labeled. Residues in Site 1 that interact with EPObp are shown in yellow; residues in Site 2 are coloured in orange. Residues identified as biologically important to Site 1 (Lys45, Asn147, Arg150, Gly151) and Site 2 (Arg14, Tyr15, Ser100, Arg103, S104, Leu108) are displayed as space filling atoms at each site (Syed et al., 1998). This diagram was generated from the PDB accession code 1EER using RASMOL.

as high affinity (K_d~1 nM) and low affinity (K_d~1 μM) binding sites and are referred to as Site 1 and Site 2, respectively (Philo et al., 1996). Site 1 and 2 interact with the six EPObp loops connecting the β-strands from both domains: L1, L2 and L3 (D1 domain); L4 (helical polypeptide linker); and L5 and L6 (D2 domain) (Syed et al., 1998). Residues from all six loops are involved in the Site 1 interface and all except the fourth loop participate at Site 2. Site 1 is made up of EPO residues from helices A, B', D and part of the AB loop (Syed et al., 1998). It has a central hydrophobic binding pocket surrounded by hydrophilic interactions. Phe93 on loop L3 of EPObp plays the largest role in the nonpolar interactions. It is held firmly in place by hydrogen bonding to Thr44 and Asn147 of EPO. Site 2 is largely made up of EPO residues from helices A and C and interacts with a relatively flat hydrophobic surface on EPObp. Phe93 of EPObp is also a major contributor to the Site 2 hydrophobic binding site. Site 1 contains almost twice as many sidechain-sidechain interactions as Site 2 which likely accounts for the difference in receptor affinity. The sidechain interactions between Site 1 and 2 and each EPObp are predominantly between positively charged Lys and Arg residues of EPO and negatively charged Asp and Glu sidechains of EPObp (Syed et al., 1998). Although polar residues participate in most of the interactions across both interface, the hydrophobic contacts were found to make the greatest contribution to the binding affinity (Syed et al., 1998).

The crystal structure of EPO-$(EPObp)_2$ shows a buried surface area of 920 $Å^2$ for Site 1 and 660 $Å^2$ for Site 2 (Syed et al., 1998). Despite this extensive interface between EPO and its two receptors, mutagenesis studies have determined that residues important for bioactivity reside in a small subset of these residues (Wen et al., 1994; Matthews et al., 1996;

Elliott et al., 1997). This supports studies showing that although many residues that make contact at the interfaces between a cytokine and its receptor (structural epitope), the majority of the binding energy comes from a small subset of residues (functional epitope) (Wells, 1995).

II. Elucidation of Biologically Important Sites on EPO

Prior to the determination of the EPO structure, initial studies to elucidate the structure-function relationship of EPO relied primarily on the use of antibodies to map functionally important sites. Identification of functional domains of EPO included the use of monoclonal antibodies against EPO peptides (Sytkowski and Fisher, 1985) or the intact protein (D'Andrea et al., 1990), and polyclonal antibodies raised against peptides derived from the predicted hydrophilic domains of EPO (Sytkowski and Donahue, 1987). Antibodies that inhibited the biological activity of EPO implied that they had bound to a functionally important domain such as the receptor-binding site. However, this result was confounded by the fact that antibodies binding an irrelevant site could also impair bioactivity by either steric hindrance or induction of a conformational change in the receptor-binding domain (Elliott et al., 1997). At best, this method only identified potential regions, rather than specific amino acids, important for EPO function.

To study the structure-function relationship of EPO at the level of individual amino acids, the next major strategy involved observing the effects of single amino acid replacements (Wen et al., 1994; Matthews et al., 1996; Elliott et al., 1997). The point mutations in EPO were chosen based on the predicted three-dimensional structure of EPO

(Boissel et al., 1993) and each mutation mutant was evaluated for altered specific bioactivity. Substitutions of the basic amino acids (Arg 14, Arg103, Arg150 and Lys45) in EPO caused a drastic decrease in bioactivity suggesting that they played an important role in the active site. It was thus postulated that electrostatic interactions between EPO and its receptor were modulated primarily by positive charges on EPO and presumably by negative charges on the EPOR (Elliott et al., 1997). This was confirmed when the crystal structure of EPO and EPObp was solved (Syed et al., 1998).

The regions important to biological activity were mapped to two sites on EPO (Fig. 2). These regions corresponded to the high (Site 1) and low (Site 2) affinity binding sites identified in the solution and crystal structures of EPO. Residues found to be the most biologically important (i.e. functional epitope) in Site 1 included Lys45 of Helix A and Asn147, Arg150 and Gly151 of Helix D (Wen et al., 1994; Matthews et al., 1996; Elliott et al., 1997). The functional epitope of Site 2 included residues Arg14 and Tyr15 of the AB loop, and Ser100, Arg103, Ser104 and Leu108 of Helix C (Wen et al., 1994; Matthews et al., 1996; Elliott et al., 1997). Muteins with a point mutation in any of these residues caused at least a 50-fold loss of bioactivity relative to EPO.

C. New Insights into EPOR activation from Recent Structural Studies

Three crystal structures of the extracellular ligand-binding domain of human EPOR complexed with non-native ligands have recently been solved. Note that the extracellular ligand-binding domain of human EPOR is referred to as EBP in all structural studies

involving non-native ligands, whereas in its complex with EPO, it is referred to as EPObp. Each structure gives new insight into the requirements of EPOR activation, challenging the idea that simple dimerization of the receptors is sufficient for activation. These studies reveal that homodimerization is required but is not sufficient for activating the receptor and that changes in the relative orientation of the receptor monomers play an important role in this process. In addition, the ability of the EPOR to bind multiple non-native ligands demonstrates the plasticity or flexibility of the receptor-binding site which increases the probability of other designed molecules binding to the receptor.

I. Homodimerization required for EPO activation

a. Discovery of EPO mimetic peptides (EMPs)

The earliest evidence that the ligand-binding site of EPOR was able to recognize non-native ligands came with the discovery of a set of EPO mimetic peptides (EMPs). This family of peptides, with no sequence or structural homology to EPO, emulated the biological properties of the native ligand, EPO (Wrighton et al., 1996). Initial screening of random phage display peptide libraries against the immobilized extracellular domain of EPOR identified a cyclic peptide, GGCRIGPITWVCGG, that exhibited EPOR-binding activity (Wrighton et al., 1996). Libraries centered around this initial lead peptide led to the production of a family of agonist peptides, 20 amino acids in length (Wrighton et al., 1996). These peptides were cyclic due to the presence of a disulfide bond and had a minimum consensus sequence of **YXCXXGPXTWXCXP**, where X was occupied by one of several amino acids. The most well characterized peptide was EMP1; its sequence was GGT**YSCHF**G**PLTWVCKP**QGG (letters in bold type represent conserved amino acids

within the family of peptides). This peptide competed with EPO in receptor-binding assays, caused proliferation of cell lines engineered to be responsive to EPO, and induced phosphorylation patterns identical to those of EPO. EMP1 also caused erythroid colony formation of cells cultured from human and murine bone marrow as well as human peripheral blood. Furthermore, two *in vivo* models of nascent red blood cell production were tested which demonstrated that EMP1 was able to elicit an erythropoietic response in mice (Wrighton et al., 1996). Taken together, this data showed that the small peptide agonist, EMP1, whose amino acid sequence was unrelated to EPO, could bind to and induce a biologically active conformation or assembly of EPOR. Concurrent structural studies of EMP1 bound to EBP showed that homodimerization was responsible for receptor activation and subsequent signaling activity (Livnah et al., 1996).

b. EMP1-EBP structure

The first ligand-receptor complex described for EPOR was the 2.8 Å crystal structure of EMP1 bound to EBP expressed in *E. coli* (Livnah et al., 1996). A noncovalent dimer of the EMP1 peptide was seen to occupy a cleft formed between the ligand-binding regions of two EPOR (Fig. 3). Each EMP1 peptide interacted with the other EMP1 peptide and with both receptor molecules at virtually identical binding sites due to a two-fold symmetrical assembly (Fig. 3).

Each EMP1 peptide had a hairpin structure consisting of two short anti-parallel β-strands connected by a disulfide bridge at one end and a slightly distorted type-I β-turn from the GPXTW region (Gly9-Pro10-Leu11-Thr12) at the other (Livnah et al., 1996). The

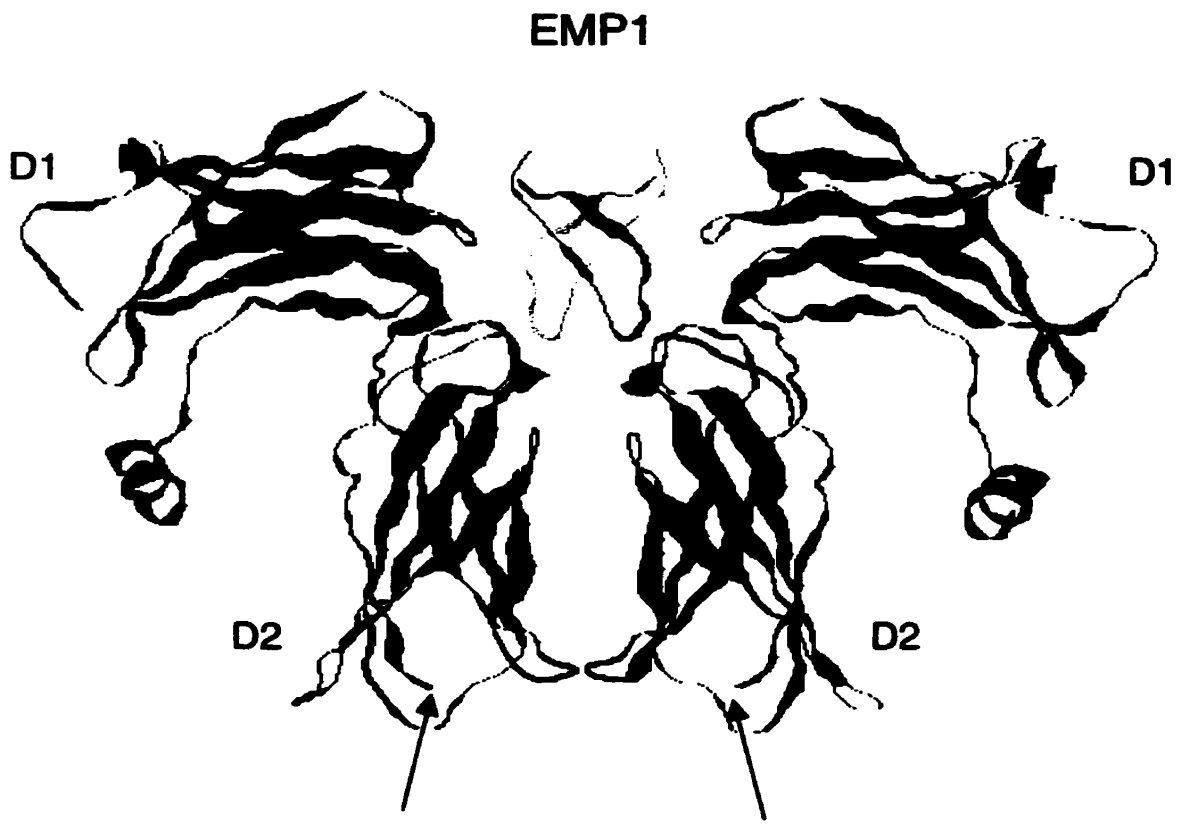

Fig. 3 Crystal Structure of EMP1-EBP complex

Ribbon diagram of the EMP1-EBP complex. The two EBP molecules are shown in blue and green, and the noncovalent dimeric peptide ligand is displayed in yellow and red. Two EMP1 peptides bind two EBP receptor molecules in a symmetrical manner. The EBP domains are labeled D1 and D2, and the membrane-proximal ends of each receptor are indicated by an arrow. This figure was made in RASMOL using the PDB accession code 1EBP.

complex revealed that each EMP1 peptide interacted with the loop regions (L1, L3, L5, and L6) of each receptor monomer either through peptide backbone hydrophobic interactions of the GPXTW region or through a hydrogen bond contributed by the peptide side chain hydroxyl of Tyr4. Hydrophobic and polar interactions were found to mediate the EMP1-EBP interaction (Livnah et al., 1996). At the interface between one EMP1 peptide and the receptors, a hydrophobic core formed between the side chains of Phe93 (L3), Met150 (L5) and Phe205 (L6) from one EBP molecule, Phe8 and Trp13 of one EMP1 peptide, and Tyr4 and Cys15 of the other EMP1 peptide. The main polar interactions were made between the mainchain β-turn residues (Gly9, Pro10 and Leu11) from one EMP1 peptide, and the mainchain and sidechain residues in loop L5 (predominantly Thr151) of EBP. The EMP1-EBP dimer assembly was the primary interaction that mediated receptor dimerization since the receptor–receptor contact area was negligible (75 $Å^2$) compared to each EMP1–receptor-binding site interaction (420 $Å^2$) (Livnah et al., 1996).

c. Increased potency of EMP1

While EMP1 was found to mimic EPO bioactivity, its potency or efficiency of receptor activation was much lower than the native ligand EPO. *In vitro* cell proliferation assays showed that the concentration needed to elicit a 50% response in cell proliferation (ED_{50}) was 400 nM and 0.01 nM for EMP1 and EPO, respectively (Wrighton et al., 1996). Inefficient formation of the noncovalent EMP1 dimer was suspected to cause the decrease in potency (Wrighton et al., 1997; Johnson et al., 1997). Consequently, two studies involving covalently linked EMP1 dimers were carried out to determine their effect on the efficiency of activation. The first study involved chemically linking two EMP1 molecules together using a

C-terminal lysine residue as the branchpoint (chemical dimer) (Wrighton et al., 1997); the second study used a bifunctional polyethylene glycol (PEG) molecule to join two peptides through their N-terminus (EMP1 PEG) (Johnson et al., 1997). These dimers were subjected to the same biological assays as the EMP1 (monomer) peptides. The covalently linked EMP1 dimers displayed a significant increase in their ability to bind cell surface EPOR which was similar to the affinity between EPO and EPOR (Wrighton et al., 1997; Johnson et al., 1997). Despite the equivalent binding affinity for the receptor, the efficiency in receptor activation, as shown by cell proliferation, was still orders of magnitude less than EPO (ED_{50} for the EMP1 PEG dimer, chemical dimer and EPO was 2 nM , 1nM, and 0.01 nM, respectively). Furthermore, *in vivo* studies showed that the covalently linked EMP1 dimers were still at least ~4000-fold less potent than EPO (Barbone et al., 1999). While the covalently linked dimers increased the potency of EPOR activation, it was evident that homodimerization alone could not account for the large differences in efficiency of EPOR activation between EMP1 and EPO.

d. EPO dimers activate EPOR through homodimerization

Homodimerization and activation of EPOR has also been demonstrated by EPO dimers that were linked together by Gly residues. Each EPO molecule in the dimer contained an R103A mutation in its Site 2 binding domain. Although mutations at this position in EPO rendered it devoid of biological activity (Grodberg et al., 1993; Wen et al., 1994; Matthews et al., 1996), R103A EPO retained the ability to bind tightly to its receptor, presumably through its Site 1 binding domain (Matthews et al., 1996). Two R103A EPO were attached through a flexible Gly linker to generate an R103A EPO dimer. Although the monomeric

R103A EPO could not elicit biological activity, formation of R103A EPO dimers restored activity. The restored bioactivity of the R103A EPO dimer was the result of the active Site 1 binding domain of one R103A EPO molecule compensating for the deficient Site 2 receptor-binding domain of the other covalently linked R103A EPO. This indicated that two domains on the EPO molecule were needed for biological function and supported the notion that homodimerization of EPOR was required for receptor activation. Interestingly, monomeric EPO was significantly more active than the R103A EPO dimer.

From the EMP1 and R103A EPO dimer studies, it is evident that homodimerization alone cannot account for the large differences in the efficiency of EPOR activation between the synthetic molecules and EPO. This has led to the idea that the orientation of the EPOR subunits might play an important role in receptor activation. EPO, an asymmetrical molecule, would likely orient two EPOR differently than symmetrical molecules such a noncovalent EMP1 dimer and the R103A EPO dimer. This potential difference in receptor orientation could possibly account for the vast differences in their efficiency of EPOR activation.

II. Receptor orientation plays an important role in EPOR activation

a. Non-productive receptor complex

Insight into the role of receptor orientation in productive dimerization was gained from studies that investigated the functionally important amino acids in EMP1. Tyr4 was identified to play a critical role in peptide-mediated receptor dimerization (Johnson et al., 1998). To assess the role of Tyr4, a set of EMP1 analogues at this position was constructed

(Johnson et al., 1998). One of these analogues (EMP33) contained a substitution of 3,5-dibromotyrosine at the Tyr4 position. Although EMP33 could not activate EPOR, as seen by the absence of early signaling events (tyrosine phosphorylation), it nonetheless retained the capacity to bind EPOR. Furthermore, receptor-binding and dimerization analysis revealed that this antagonist (EMP33) was capable of promoting dimer formation of EBP in solution. These results illustrated that simple homodimerization was not sufficient for activation, and that receptor orientation played a pivitol role in EPOR activation.

b. EMP33-EMP complex

Structural studies of EMP33 with EBP confirmed the ability of EMP33 to dimerize EBP. The EMP33-EBP complex was similar to the EMP1-EBP complex with a 2:2 stoichiometry of peptides to receptor subunits (Fig. 4). A comparison of the EMP33 and EMP1 structures showed high similarities between the mainchain and sidechain conformations within the disulfide bridge of these peptides but displayed some deviation at their ends, due to the substitution of 3,5-dibromotyrosine at position 4 in EMP33. Similar to the EMP1-EBP complex, the interactions between the EMP33 dimer and EBP were more extensive than those between the receptors. Thus, EMP33-EBP interactions appeared to contribute the most toward the stability of the 2:2 complex. The most significant difference between the active (EMP1) and inactive (EMP33) 2:2 complexes was the orientation of the two receptors. In the inactive EMP33-EBP dimer, the D1 domains of the two receptors were oriented 165° relative to each other when viewed along the plane of the membrane, whereas in the EMP1-EBP dimer, the D1 domains had a symmetric 180° relationship (Fig. 5b and 5c) (Livnah et al., 1998). This 15° rotation in the D1 domain of the inactive 2:2 complex

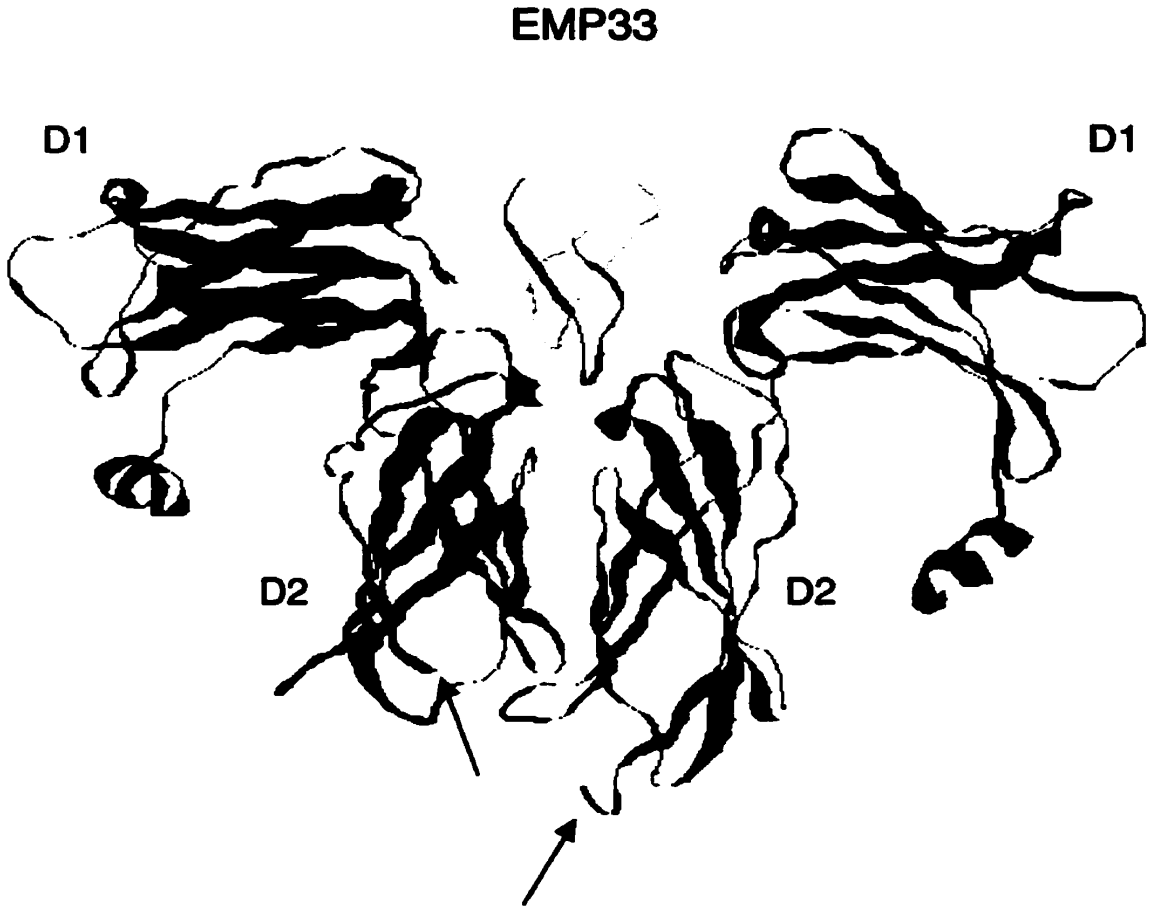

Fig. 4 Crystal Structure of EMP33-EBP complex

Ribbon diagram of the EMP33-EBP complex. The two EBP molecules are shown in blue and green, and the dimeric peptide ligand is displayed in yellow and red. Two EMP33 peptides bind two EBP receptor molecules in an asymmetrical manner. The domains are labeled D1 and D2, and the membrane-proximal ends of each receptor are indicated by an arrow. This figure was made in RASMOL using the PDB accession code 1EBA.

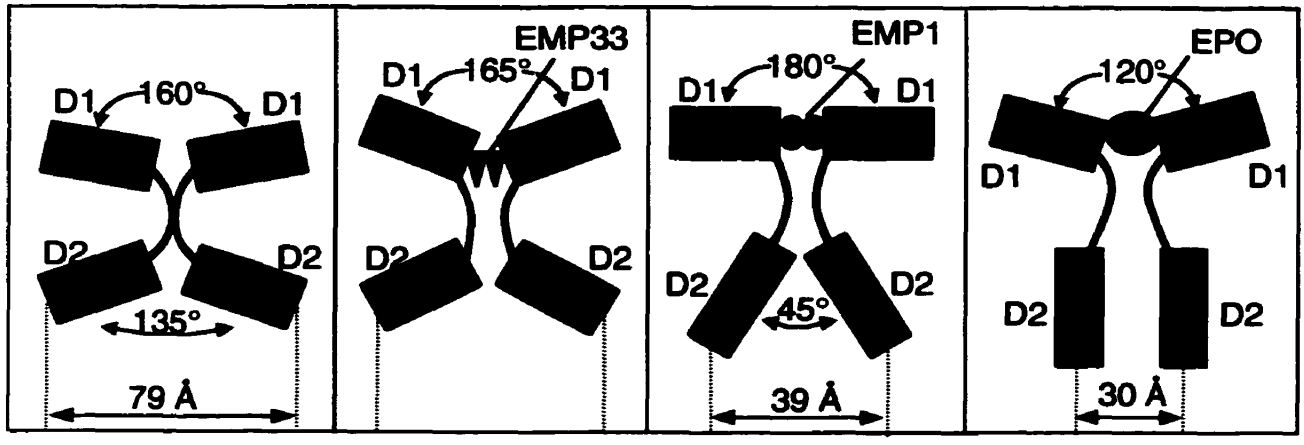

Fig. 5 Relative Orientations of EBP bound to various ligands

Relative orientations of the EBP when dimerized in (a) unliganded, (b) EMP33-liganded, (c) EMP1-liganded and (d) EPO-liganded states. The angles of the relative D1 and D2 positions are indicated. The plane of the membrane is orthogonal to the paper at the carboxyl termini of the D2 domains. Dashed lines project from the carboxyl termini of the D2 extracellular domains through the membrane identifying the distance by which the two transmembrane domains are separated in each complex. Note that the two D2 domains are aligned and separated differently depending on the relative orientations of D1, which is based on either a self-association in the unliganded form or various ligands binding EBP.

into a twist of the D2 domain (and the intracellular components) which was enough to prevent JAK2 activation (Wilson and Jolliffe, 1999). This may have represented a possible limit in the orientation of the D2 domain needed for signaling. Crystal structures of six other active EBP-peptide complexes revealed a two-fold symmetric dimer configuration similar to that found in the EMP1-EBP complex (Livnah et al., 1998). The inactive EMP33 peptide was the only peptide found to have an asymmetric mode of dimerization (Livnah et al., 1998). Interestingly, examining the orientation of the EPO-$(EPObp)_2$ complex revealed a highly asymmetric assembly of the receptors. As seen in Fig. 5d, the D1 domains of each receptor molecule were oriented at ~120° relative to each other.

The ability of EMP33 to dimerize EPOR, but not cause activation, confirms the view that simple homodimerization is not sufficient for receptor activation. Although two receptors were brought equally close to each other in the EMP1-EBP, EMP33-EBP and EPO-$(EPObp)_2$ complexes, differences in their relative orientations led to drastic differences in their ability to elicit a growth signal.

c. Biological studies support importance of receptor orientation in EPOR activation

Most of the early work that involved dissecting the mechanism of cytokine regulation suggested that bringing two receptors into close proximity to one another was sufficient for signal transduction. The following findings support this hypothesis: (i) EPOR mutants containing a Cys mutation in its D2 domain (enabling two receptor molecules to form a disulfide bond) were found to be constitutively active (Watowich et al., 1992), (ii) Bivalent monoclonal antibodies (IgG) raised against EBP could activate EPOR (Elliott et al., 1996),

and (iii) Expression of a purely antagonist EPO mutant (R103A EPO) as single-chain dimers yielded agonists (Qiu et al., 1998). Undoubtedly, a broad variation in structures must have accompanied this array of receptor dimers. These results suggested that activation was fairly insensitive as to how the intracellular chains and associated JAKs were brought together.

However, in light of recent structural data, a closer examination at these studies suggests that EPOR activation is tightly controlled by receptor orientation. In the case of EPOR mutants with Cys mutations, only a limited number of point mutations, R129C, E132C, E133C (murine) (Watowich et al., 1994), R130C (human) (Livnah et al., 1998), were able to form a disulfide bond and activate the receptor. The limited number of permissive positions for the Cys residue suggests that only a limited number of permissive EPOR arrangements lead to a productive dimer configuration. Furthermore, in the case of the bivalent antibodies, only 4 out of the 96 anti-EPOR antibodies were capable of eliciting a proliferative response and these did so with substantially lower activities than could be achieved with EPO (Elliott et al., 1996). The IgG molecule has considerable flexibility at the hinge region thus allowing it to make adjustments to bind and dimerize EPOR. The small percentage of anti-EPOR antibodies that were able to activate the receptor provided further support that only a limited number of EPOR dimeric orientations exist that result in constitutive activation.

Re-examining previous studies together with the EMP33 data provide basis to the proposal that simple homodimerization is not sufficient for receptor activation and that the orientation of the receptors play a large role in conferring optimal biological activity. The

discovery of the peptide agonist- and antagonist-receptor complexes suggests that subtle changes in the orientation of the cell surface receptor monomers are responsible for an 'on' or 'off' switch for receptor signaling activity in the cytoplasm.

III. EPOR activation: Receptor Orientation in the context of Preformed Dimer?

a. Structure of Unliganded EBP

Despite extensive evidence for ligand-induced dimerization, Livnah et al. (1999) found unexpectedly that the unliganded EBP crystallized as a cross-shaped dimer (Fig. 6). The interface between the receptors involved more than 20 residues from five of the six binding loops (L1, L3, L4, L5, and L6). Notably, these were the same residues used to bind EPO (Syed et al., 1998), EMP1 (Livnah et al., 1996) and EMP33 (Livnah et al., 1998). The most distinctive feature of the unliganded EBP was the distance between C-terminal (membrane-proximal ends of D2) residues and hence, the distance between the two transmembrane domains. This distance corresponded to 73 Å and was a result of the two D2 domains being oriented away from each other at an angle of 135° (Fig. 5a). In contrast, the D2 domains of the EMP1-EBP dimer were oriented away from each other at an angle of 45° separating the transmembrane domains by 39 Å (Fig. 5c) (Livnah et al., 1999). The D2 domains of the EPO-$(EPObp)_2$ complex were parallel to each other and inserted perpendicular to the membrane resulting in the transmembrane domain being separated by only 30 Å (Fig. 5d) (Syed et al., 1998). The EBP-EBP dimer configuration appears to keep the intracellular ends sufficiently far apart to prevent autophosphorylation of the associated JAK2 molecules and downstream signaling. Ligand-binding would induce close dimer association of the D2 domains, possibly by a scissor-like motion, and allow interaction of

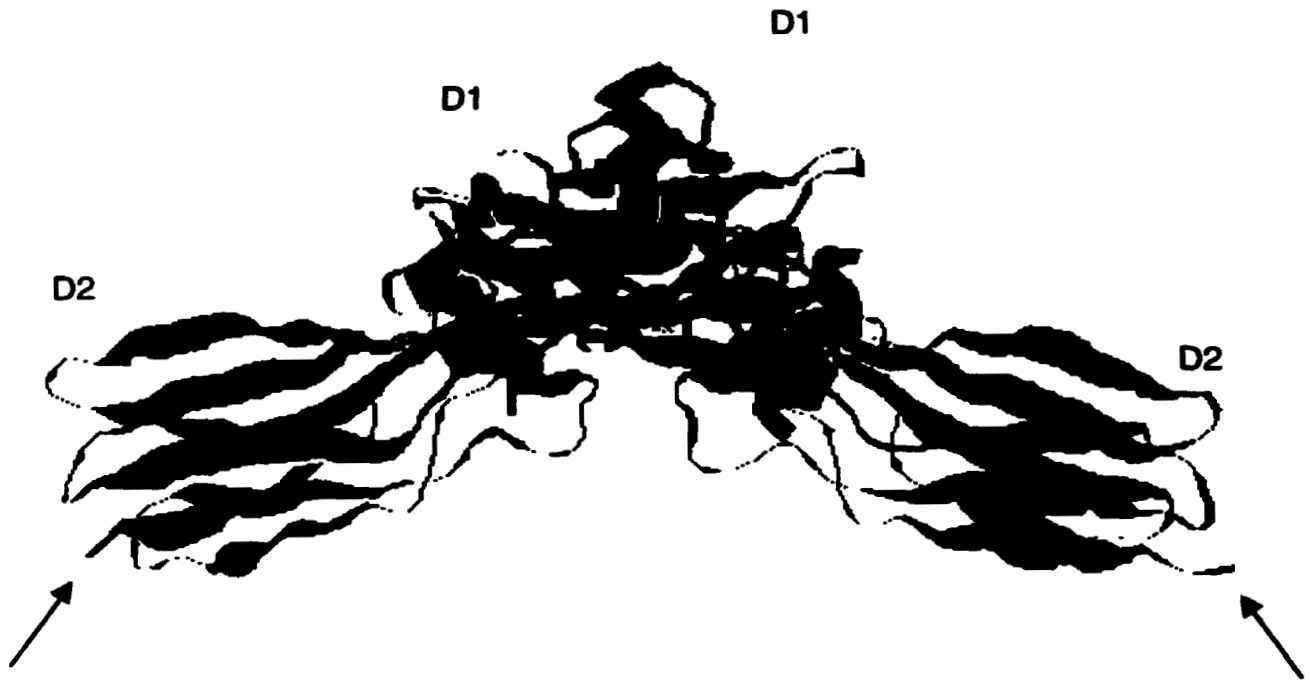

Fig. 6 Crystal Structure of Unliganded EBP

Ribbon diagram of EBP-EBP complex viewed along to the plane of the plasma membrane. The two EBP molecules form a cross-like self dimer and are shown in blue and green, with their individual domains labeled D1 and D2. The D1 domains of each monomer point in opposite directions, whereas the two D2 domains are aligned toward the membrane with a 135° between them. The membrane-proximal ends of the D2 domains in each molecule are shown by an arrow, emphasizing the 73Å separation between them. This figure was made in RASMOL using the PDB accession code 1ERN.

their intracellular domains, resulting in signaling (Livnah et al., 1999).

b. Biological relevance of Preformed EPOR dimers

A fluorescent protein fragment complementation assay was used to test the biological relevance of the EBP dimer crystal structure (Remy et al., 1999). The basis of this assay was that two complementing fragments of the enzyme dihydrofolate reductase (DHFR), when fused to two separate but interacting proteins, would reassemble and regain its ability to bind to a fluorescent molecule. When DHFR fragments were fused onto the end of the full-length EPOR, the same level of fluorescence was observed in the presence or absence of ligand. Remy et al. (1999) claimed that their results supported the case that distinct dimeric conformations of unliganded EPOR existed on living cells (Remy et al., 1999). However, their experimental approach raised some concerns. First, the intrinsic affinity between the two complementary DHFR fragments was not reported. A high affinity between the two fragments would have contributed to the fluorescent signal and complicated the interpretation of their results. This could have been determined by observing the interaction of the two fragments in solution. Second, the affinity of the two fragments linked to known non-associating membrane proteins could have been determined to assess whether the two fragments had a tendency to associate when constrained to a membrane protein. The two fragments would be attached to the membrane proteins by a linker similar in length to the cytoplasmic domain of EPOR. Any tendency for the two fragments to reassemble would serve as a background fluorescent signal and would need to be considered when interpreting the results of their experiments.

c. Role of Preformed EPOR Dimers

In the context of the surface of a cell, it is unclear whether any or all receptors exist as preformed dimers. The structural and biological data of the unliganded EBP seem to contradict biophysical studies (sedimentation equilibrium and size exclusion chromatography with on-line light scattering detection) that show that in solution, EBP does not self-associate into dimers or higher oligomers (Philo et al., 1996). However, Philo et al. (1996) contended that from the results of their biophysical studies, the binding interaction of the receptor alone, when stimulated by EPO, was probably insufficient to explain the efficiency of receptor activation under physiological conditions (Philo et al., 1996). Factors suggested to play a role in this event included the presence of clustered receptors on the cell surface, weak interactions of the transmembrane and intracellular domains of the receptors, and other unidentified cellular components (Philo et al., 1996). Although weaknesses exist in the evidence for preformed receptor dimers, a self-associating EPOR dimer would function similarly to the clustering of receptors, accounting for the potent biological response to EPO from cells with fewer than 1000 EPOR present (Broudy et al., 1991). Preformed dimers would facilitate the formation of ligand-receptor complexes by increasing the effective receptor concentration. This is important to the sequential dimerization of the EPO-EPOR interaction (Matthews et al., 1996) where the first receptor subunit binds EPO with a high affinity and then the second receptor subunit binds EPO with a much lower affinity (Philo et al., 1996). An expected weak association (millimolar range) of the truncated soluble, extracellular cell surface receptor could explain the lack of detection of EPOR dimers (in the absence of ligand) in biophysical studies. A dissociation constant for EPOR as high as 50 mM could translate into micromolar range affinities on the cell surface as a result of two-

dimensional lateral diffusion and increased stability of the full-length receptor containing the transmembrane domain (Philo et al., 1996). Further studies will need to be carried out to definitively determine if preformed EPOR dimers exist on the surface of a cell.

IV. Plasticity of the Receptor

As mentioned earlier, the native EPO molecule has two different binding sites with which to bind and activate its receptor. However, various non-native molecules have been shown to activate the receptor, demonstrating the plasticity or flexibility of the EPOR ligand-binding site. The following molecules have been shown to activate EPOR: (1) a dimeric EPO containing only one binding site on each monomer (R103A EPO), (2) symmetric EPO mimetic peptides (e.g. EMP1), (3) mutant EPORs which are crosslinked by a disulfide bond (EPOR with a R103C mutation), and (4) bivalent antibodies raised against the extracellular portion of EPOR. Both asymmetric and symmetric molecules have been found to activate EPOR. Orientation of two EPOR by these ligands results in a wide range of intermediate activity states.

Although EPOR exhibits flexibility in its ligand-binding site (to bind different ligands), the residues that participate in binding the different ligands are the same. Residues Phe93 in loop L1 and Phe205 in loop L6 of EPOR were found to be important for binding to both EPO and EMP1 (Middleton et al., 1999). Furthermore, these residues were also observed in the buried surface of the EMP33-EBP and EBP-EBP crystal structures. This suggests that Phe93 and Phe205 make up a minimal functional epitope on EPOR that contributes greatly to binding (Wilson and Jolliffe, 1999). It appears that the receptor-

binding site does not change substantially in order to accommodate the various ligands; only relatively small changes in the loops or in the orientation of the sidechains are required for interaction with different molecules.

D. Rationale for using EPO as a model cytokine

The aim of this thesis is to examine a general method for designing antagonists of helical cytokines using EPO as a model cytokine. An antagonist can be defined as a molecule that inhibits the ability of a cytokine to cause intracellular events that ultimately lead to proliferation, differentiation or apoptosis. Although inhibiting the action of a hormone can occur extracellularly or intracellularly, the scope of the present work is to design antagonists to bind the extracellular portion of the helical cytokine receptor. Activation of cytokine receptors, which lead to downstream signaling events, involve oligomerization of at least two receptors. Therefore, designing molecules that bind one receptor would inhibit the ability of the natural ligand to dimerize or oligomerize the receptor complex. EPO was chosen as the model cytokine because it is exemplary of the structure of other helical cytokines. In addition, its receptor, EPOR, resembles that of other helical cytokine receptors and therefore, EPO bound to one EPOR can represent the molecular recognition of other helical cytokines with one of their cognate receptors (Bazan, 1990; Wells and de Vos, 1996).

I. Helical cytokine structures are similar to EPO

EPO belongs to a family of hormones and receptors known as the class I

hematopoietic or cytokine superfamily (Bazan, 1990) that govern a number of immune and growth functions. This family of proteins include growth hormone (GH), prolactin (PRL), erythropoietin (EPO), granulocyte- and granulocyte-macrophage colony-stimulating factors (G- and GM-CSF), thrombopoietin (TPO), leukemia inhibitory factor (LIF), stem cell factor (SCF), ciliary neurotrophic factor (CNTF), IL-2, IL-3, IL-4, IL-5, IL-6, IL-7, IL-9, IL-11, IL-12, IL-13, and IL-15, and is linked by several common structural and functional features (Wells and de Vos, 1996).

Although the members of this superfamily share low homology at the amino acid level, these cytokines share similar secondary and tertiary structures. The structures of EPO (Syed et al., 1998), GH (de Vos et al., 1992), G-CSF (Aritomi et al., 1999), GM-CSF (Walter et al., 1992), LIF (Robinson et al., 1994), CNTF (McDonald et al., 1995), and IL-2 through IL-6 (Brandhuber et al., 1987; Feng et al., 1996; Muller et al., 1995; Milburn et al., 1993; Somers et al., 1997) have been solved by either NMR or X-ray diffraction and a theoretical model has been deduced for PRL (Halaby et al., 1997). Examining these structures reveal remarkably similar topological folds. Fig. 7 shows the general topology of these cytokines. Each ligand is made up of helices A, B, C and D where helices A and D pack against B and C. The helices are arranged in a left-handed 4-helix bundle such that helices A and B run in the same direction and C and D in the opposite direction. Linking the helices in this arrangement is made possible by a long loop joining the A and B helices, a short one between B and C and a second long connection between helices C and D. Of all the solved and predicted structures, CNTF is the only cytokine that has a slightly different helix arrangement in which Helix C replaces D and vice versa (McDonald et al., 1995). Differences between

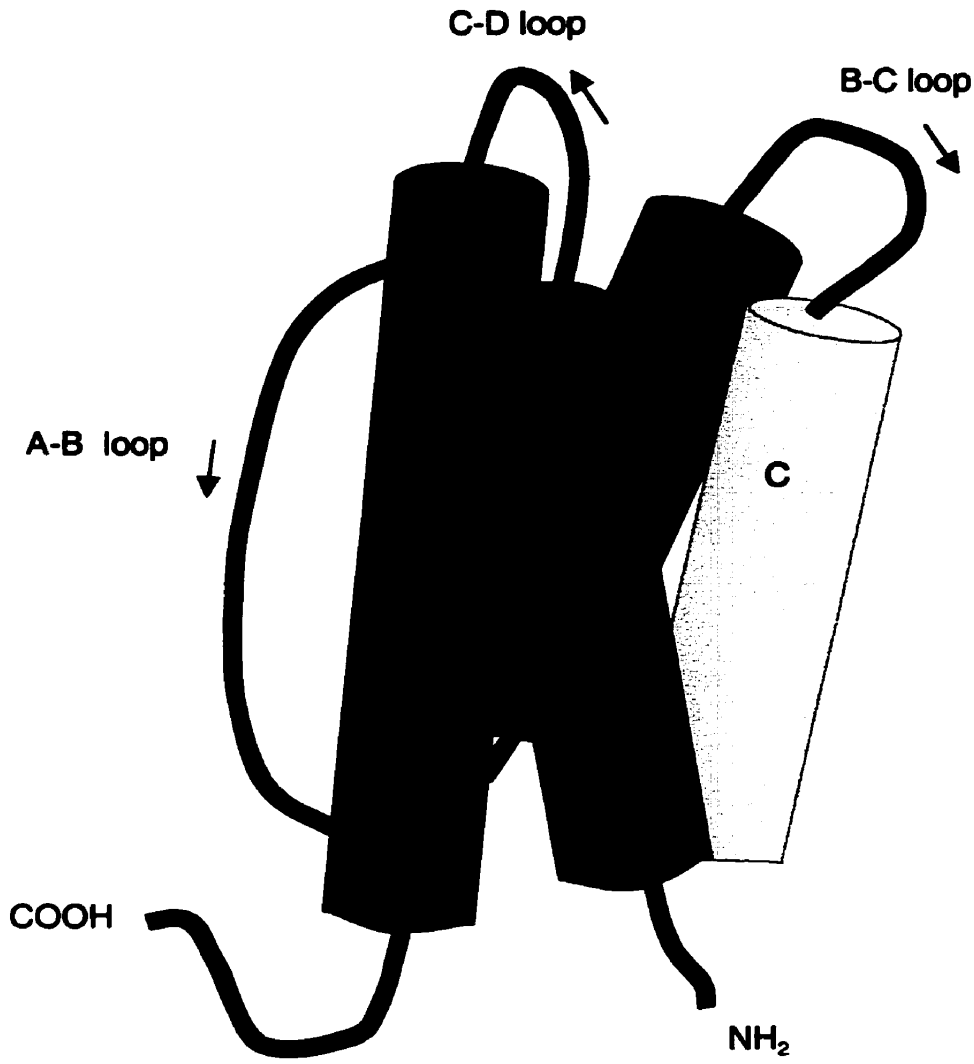

Fig. 7 Schematic of a generic 4-helix bundle

Schematic of a generic 4-helix bundle. This diagram represents the structure of the cytokines belonging to the Class I hematopoietic superfamily. Helices (A, B, C, and D) and the loop connectivities are labeled.

the various cytokine structures include the relative lengths of the helices, the lengths and nature of the various connecting elements (e.g. small helical segments or β-strands), and the pattern and number of disulfide bonds. However, despite these differences, Fig. 8 clearly shows that the prevailing common element that links this group of cytokines to the same family is their 4-helix bundle structure. This common structure supports the use of EPO as a model cytokine to determine the feasibility of generating an antagonist using our method of design. The success of designing an EPO antagonist would likely translate into the success of generating other cytokine antagonists that would have therapeutic value.

II. Helical cytokine receptor structures are similar to EPOR

Aside from the structural similarities between the ligands of the class 1 cytokine superfamily and EPO, the cognate receptors of this family also share structural similarities with EPOR. Analogous to EPOR, each receptor of this family has an extracellular domain, a single transmembrane segment and a cytoplasmic domain. The distinctive feature of the hematopoietic receptor family member is the presence of a conserved cytokine receptor homology (CRH) region within the extracellular portion, which is usually involved in hormone binding (Wells and de Vos, 1996). Each of the CRH domains consists of 200-250 residues and has two fibronectin (FBN) type III domains connected by a short helical linker. Each domain contains seven β-strands and is divided into two sheets. The two domains of the receptor are positioned such that it exposes the loops at the end of the domains so that residues in the loops can bind the hormone. Thus, each receptor interacts with a cytokine using the hinge regions (between the two domains) and the exposed loops (Fig. 9). These

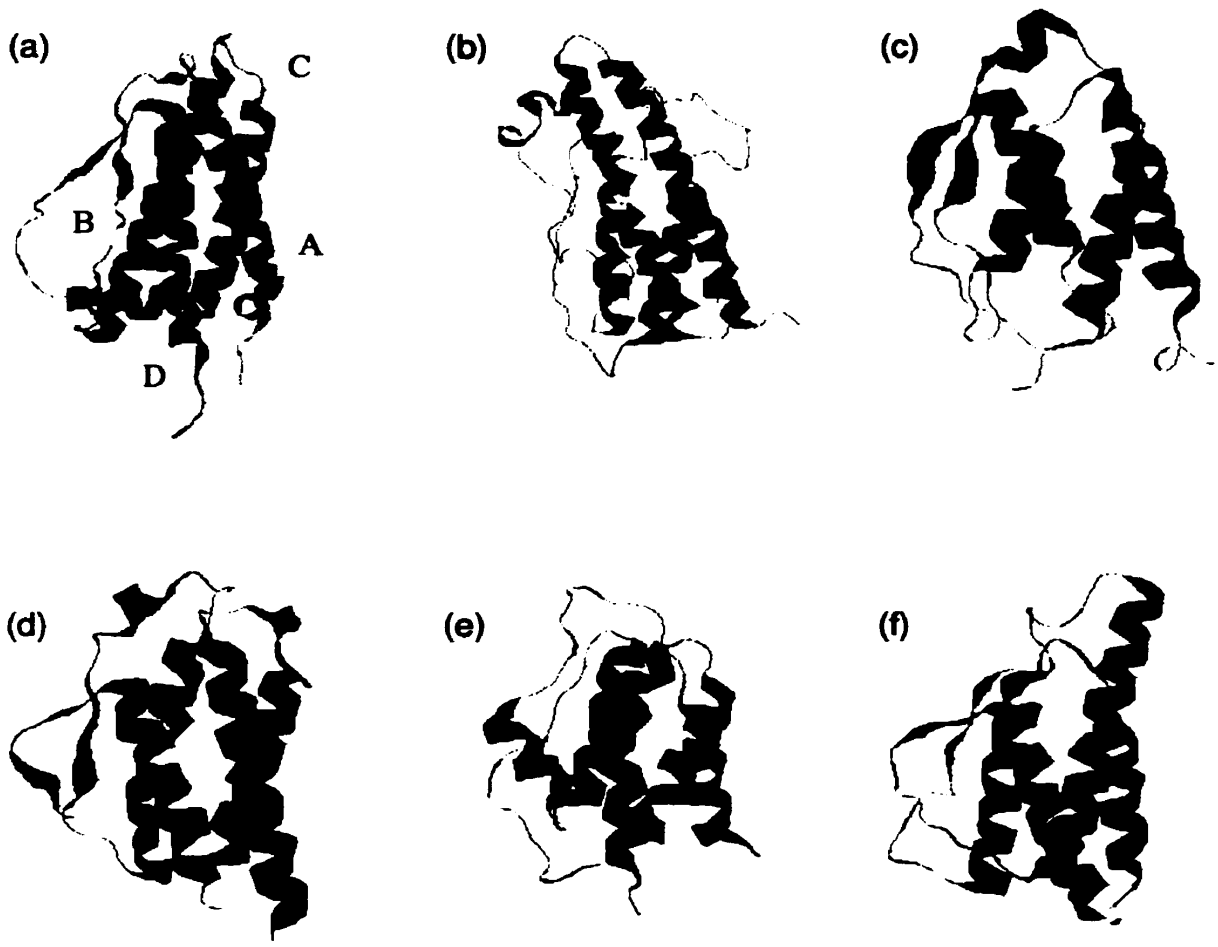

Fig. 8 Crystal Structure of Various Hematopoietic Cytokines

Three-dimensional structures of various hematopoietic cytokines. All helices are 4-helix bundles. Helices are labeled A, B, C and D on EPO. Helices A and D are coloured in blue and helices B and C are coloured in green for all cytokines. (a) EPO; PDB accession code is 1EER, (b) GH; PDB accession code is 1HGU, (c) GM-CSF; PDB accession code is 1CSG, (d) IL-2; PDB accession code is 3INK, (e) IL-3; PDB accession code is 1JLI, and (f) IL-4; PDB accession code is 1HIK. These figures were made using RASMOL.

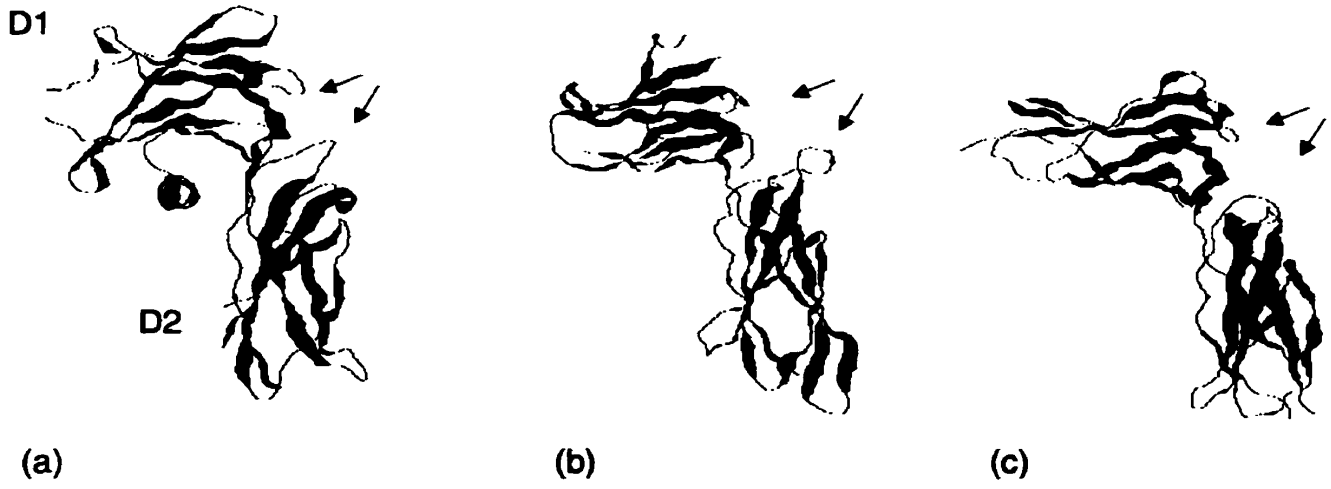

Fig. 9 Crystal Structure of Various Hematopoietic Cytokine Receptors

Crystal structures of the extracellular domains of EPOR, GH receptor and G-CSF receptor. The two FBN type III domains of EPOR are labeled D1 and D2. The ligand-binding site on each receptor is identified by arrows. Note that all receptors have similar structure. (a) EPOR; PDB accession code is 1EER, (b) GH receptor; PDB accession code is 3HHR, and (c) G-CSF receptor; PDB accession code is 1CD9. This figure was generated using RASMOL.

domains correspond to the D1 and D2 domains of EPOR mentioned earlier in this chapter. The structural similarities of the receptors of this family are evident from the crystal structures of the extracellular domains of EPOR, GH receptor, and G-CSF receptor (Fig. 9). This further supports using EPO to represent this family of cytokines in the design of antagonists to their receptors.

III. Cytokines activate cognate receptors similar to EPO activating EPOR

It has been well established that oligomerization of EPOR by EPO plays an important role in receptor activation. Cytokines of the class I superfamily activate their cognate receptors in a similar manner. The oligomeric structure of the hematopoietic receptor-signaling complex can be divided into two categories, the homodimeric and hetero-oligomeric groups (Wells and de Vos, 1996). Cytokines like EPO, GH, and PRL belong to the homodimeric group. For this group, the α receptor subunit that binds the hormone is responsible for signaling. This α receptor contains the CRH domain and for EPOR, is equivalent to its extracellular domain. The hetero-oligomeric group, of which IL-4 and IL-6 are good examples, have at least two receptors (α and β); the α receptor is generally responsible for binding the hormone and the β receptor is responsible for signaling (Wells and de Vos, 1996). Regardless of which category the receptor-signaling complex belongs to, both groups utilize an α receptor subunit in binding the receptor. The interaction of the helices of a cytokine with its α receptor is analogous to EPO binding to its α receptor subunit and is the interaction of interest for designing antagonists.

In summary, it is evident that the three-dimensional structure of EPO is analogous to

the structure of the other cytokines of the class I cytokine superfamily. Its receptor, EPOR, is also similar in structure to the receptors of this family. Furthermore, EPO binds to EPOR, an α receptor subunit, to initiate signal transduction; an α receptor subunit is also involved in receptor activation by other cytokines of this family. Therefore, the interaction between EPO and EPOR can represent cytokine-receptor complexes where the cytokine is helical, at least one of its receptors is composed of two FBN type III folds linked together by a small helical linker, and where the interaction between the cytokine and receptor involves the loops of the FBN domains.

E. Aim of the Study

In the present work, we have set out to design antagonists of helical cytokines using EPO as our model cytokine. Our method involves grafting short amphipathic segments of a cytokine onto a helical scaffold to produce a 3-helix bundle. Designing small helical proteins with a specific function has the potential for success for the following reasons. Studies involving the growth hormone complexed with its receptor have revealed that relatively few residues within the large cytokine-receptor contact surface are needed to achieve binding (Wells, 1995). This suggests that nature has not produced the smallest protein domains possible for discrete functions; an attribute that is advantageous to designing small binding molecules. In addition, extensive work has been carried out on the design of helical bundles, demonstrating the understanding of the basic concepts of bundle formation (Bryson et al., 1995; Kamtekar et al., 1993). Moreover, there has been success in designing 3- and 4-helix bundles that possess native-like characteristics (Regan and DeGrado, 1988; Walsh

et al., 1999).

Although an EPO antagonist has limited therapeutic value because most diseases require the administration of rhEPO (Foa, 1991), the similarities in structure between EPO and other cytokines, and between EPOR and other cytokine receptors, provide a rational basis for using EPO to test our method of designing antagonists to helical cytokines receptors. Furthermore, the abundance of structural and biological data on EPO, EPO mimetics, and EPOR, combined with the availability of necessary reagents, provides a solid foundation for this work. The crystal structure of EPO has indicated the structural sites used to bind the receptor, and mutagenesis data has led to the identification of specific residues important to biological activity. This allows one to be in a better position to rationally design small molecules that mimic the natural ligand-receptor interface and will provide a framework from which to design an antagonist to EPOR.

Chapter 2: Cytotoxicity of Designed Peptides based on the Human Erythropoietin Sequence

This chapter appears in the form of the manuscript that will be submitted. The figures, figure legends, and tables have been placed in the body of the text.

Cytotoxic Activity of Designed Peptides based on the Human Erythropoietin Sequence

Cynthia S. Quan‡, Douglas Cossar†, Dwayne L. Barber§, and Avijit Chakrabartty‡*

‡Department of Medical Biophysics and §Department of Laboratory Medicine and Pathobiology, University of Toronto, Toronto, Ontario, Canada, M5G 2M9

§Department of Laboratory Medicine and Pathobiology, Toronto General Hospital, University Health Network, Toronto, Ontario, Canada, M5G 2C4

†Cangene Corporation, 3403 American Drive Mississauga, Ontario, L4V 1T4

Running Title: Cytotoxic Erythropoietin-based Peptides

* To whom correspondence should be addressed: Ontario Cancer Institute, Division of Molecular and Structural Biology, 610 University Ave., Toronto, Ontario, M5G 2M9, Canada, Phone: (416) 946-4501 Ext. 4910; Fax: (416) 946-6529; Email: chakrab@oci.utoronto.ca

Abstract

The design of helical cytokine antagonists can lead to the development of drugs that can treat a variety of diseases ranging from rheumatoid arthritis to cancers. In this study, we set out to develop a general method for designing antagonists of helical cytokines. Our method involved grafting short amphipathic segments of a helical cytokine, which contained residues important for its biological activity, onto a helical scaffold to produce a 3-helix bundle with molten globule structure. The molten globule nature of the designed molecules was expected to be advantageous because the flexibility in its tertiary structure would facilitate binding to the receptor. To test this strategy, erythropoietin (EPO) was used as a model cytokine. Six potential antagonists (48 residues in length) and three control peptides were designed and synthesized. Their structural characteristics were assessed by circular dichroism, and urea and thermal denaturation experiments. All antagonist peptides possessed the expected helical and molten globular characteristics. Although the designed molecules exhibited all the expected structural characteristics, the peptides lacked specific antagonist activity and did not bind the soluble EPO receptor (EPOR). However, the designed antagonist peptides showed an unexpected cytotoxic activity that varied in magnitude. The mechanism of cytotoxicity appears to be necrosis. Surprisingly, the regions of EPO grafted onto the scaffold, which confer cytotoxicity, correspond to the EPOR-binding sites of EPO. Therefore, it appears that the sequence encoding the receptor-binding sites of EPO also encodes cytotoxic activity when isolated and presented in a helical conformation.

A. Introduction

Cytokines such as erythropoietin (EPO), growth hormone, and alpha-interferon have proven to be excellent drugs for the treatment of anemia (Foa, 1991), dwarfism (Guevara-Aguirre et al., 1991), and leukemia/Kaposi sarcoma (Itri, 1992), respectively. However, their largest drawback is that they cannot be delivered orally. Therefore, development of orally active, bioavailable small molecule agonists and antagonists to cytokine receptors would be extremely beneficial.

Development of small molecule cytokines has been challenging. Currently, three general approaches are being utilized. The first strategy is rational drug design, which relies heavily on computer-assisted 3D-structure analysis of ligands, receptors, and their complexes. Computer models of non-peptide molecules that fit the receptor-binding site are constructed and docked on to the model structure of the receptor. The binding affinity of this virtual complex is evaluated using various computer programs. The small molecule ligands generated using this approach retain certain structural features of the larger natural ligand. The major drugs developed via rational drug design are the HIV protease inhibitors for the treatment of AIDS (Wlodawer et al., 1989).

The second approach involves creating and searching combinatorial libraries of small molecules for active compounds. The limitation of this approach is its requirement for a high-throughput assay that can be used to screen the libraries. Brute-force analysis, often utilizing robotics, is used to identify lead compounds that bind the receptor. A slightly different combinatorial method is phage display (Smith, 1985). In this procedure, phage

particles, displaying short unique peptides on their surface, are passed over an immobilized receptor. Phage particles that bind specifically to the receptor are eluted and amplified. Sequencing the phage DNA reveals the peptide sequence responsible for the binding activity. Small molecule ligands generated using the combinatorial approach may differ completely from the natural ligand, both in structure and in the mechanism of binding. The feasibility of the combinatorial approach was recently demonstrated through the development of short peptide agonists of the EPO receptor (Wrighton et al, 1996). In addition, small molecule agonists of both EPO (Qureshi et al., 1999) and the murine granulocyte-colony stimulating factor receptor (Tian et al., 1998) have been recently isolated.

The third approach involves the identification of functional epitopes followed by structure-based studies to design small molecule drugs. This approach was applied to the analysis of growth hormone structure and function (Wells, 1995). The method involves extensive mutational studies of cytokines and their receptors. By studying the binding characteristics of a large number of point mutants, regions of the cytokine that contribute most to the binding energy can be located; these regions are referred to as functional epitopes (Wells, 1995). The structure of the growth hormone-growth hormone receptor complex was solved (de Vos et al., 1992) shortly after the functional epitopes were mapped. Examining the structural characteristics of the functional epitopes provided an unexpected result. The functional epitope was specifically localized to a small patch of the entire surface of growth hormone that interacts with the receptor. Thus, the entire binding interface does not contribute equally to the stability of the growth hormone-growth hormone receptor complex; rather, a small subset of interface residues make the dominant contribution to the binding

energy. By identifying the functional epitopes, computer-assisted drug design can be focused on those parts of the structure that are most important for function.

In the present study, we propose a novel method for designing antagonists of helical cytokines. We have used EPO as a model cytokine to test our strategy for the following reasons. There is an abundance of mutagenesis data (Wen et al., 1994; Elliott et al., 1997), and the X-ray crystal structure of the EPO-EPOR complex is available (Syed, et al., 1998). In addition, we have specialized cell lines that can be maintained in either EPO or IL-3 (Barber et al., 1994), thus allowing the specificity of antagonist-EPOR interactions to be evaluated in the same cell line. The principal finding of our study is that our EPO-based antagonists have anti-mitogenic activity. This activity originates from a critical sequence–structure relationship; however, the designed molecules appear to operate through a pathway that is independent of the EPOR.

B. Experimental Procedures

I. Cell culture

The murine myeloid progenitor cell line, BaF3 (Palacios et al., 1985), was maintained in RPMI 1640 medium, 10% (v/v) fetal bovine serum (Sigma), 1% L-glutamine (GibcoBRL) and 50 μM 2-mercaptoethanol (Fisher Scientific) (RMPI 1640 complete media) supplemented with 100 pg/ml recombinant murine IL-3 (R&D Systems, Minneapolis, MN). BaF3 cells stably transfected with the murine EPOR gene (BaF3-EPOR (D'Andrea et al., 1991; Barber et al., 1994)) were cultured in RPMI complete media supplemented with 0.5 units/ml recombinant human EPO. The murine EPO-dependent erythroleukemic cell line, HCD-57 (Ruscetti et al., 1990), was cultured in Iscove's modified Dulbecco's medium, 20% fetal bovine serum and 50 μM 2-mercaptoethanol supplemented with 0.5 units/ml of EPO. The human megakaryoblast leukemic cell line, UT7-EPO (Komatsu et al., 1993), was maintained in Iscove's modified Dulbecco's medium, 10% fetal bovine serum, 1% L-glutamine and 50 μM 2-mercaptoethanol supplemented with 0.5 units/ml of human recombinant EPO. The murine myeloid progenitor cell line, FDCP (Dexter et al., 1980), and the murine myeloid cell line, DA3 (Ihle and Askew, 1989), were grown in RPMI 1640 complete media supplemented with 100 pg/ml murine IL-3. The cytotoxic T lymphocyte cell lines, CTLL (Gillis et al., 1977) and CTLL-EPOR (Barber and D'Andrea, 1994) were cultured in RPMI complete media supplemented with 2 units/ml murine IL-2. B9 cells (Lansdorp et al., 1986), a murine hybridoma cell line, were grown in Iscove's modified Dulbecco's medium with 5% fetal bovine serum, 1% L-glutamine, 50 μM 2-mercaptoethanol and 1 ng/ml human IL-6 (gift from Dr. A. K. Stewart, University Health Network, Toronto). A mutant NIH 3T3 fibroblast cell line, GP+E (Markowitz et al., 1988) was grown in

Dulbecco's modified Eagles's medium supplemented with 10% fetal bovine serum, 1% L-glutamine and 50 μM 2-mercaptoethanol. All cell lines were incubated at 37°C and 5% CO_2.

II. Peptide Synthesis

Peptides were prepared by solid-phase synthesis on a PerSeptive Biosystems 9050 Plus peptide synthesizer as peptide-amides on PAL-PEG-PS resin (PerSeptive Biosystems) using fluorenylmethoxycarbonyl (Fmoc) chemistry. Deprotection of the Fmoc group was achieved by using 20% piperidine in dimethylformamide. An active ester coupling procedure, utilizing O-(7-azabenzotriazol-1-yl)-1,1,3,3-tetramethyluronium hexafluorophosphate (PerSeptive Biosystems) was used. The peptides were acetylated using a mixture of 0.5 M acetic anhydride and 0.5 M pyridine in dimethylformamide for 2 h. Cleavage from the resin was achieved with a mixture of trifluoroacetic acid, thioanisole, m-cresol and ethanedithiol (81:13:1:5) cooled to 0°C with the subsequent addition of trimethylbromosilane to a final volume of 12.5% (v/v). After incubation for 15 min on ice, peptide was separated from the resin by filtration and the cleavage reaction was continued for another 2 h. The peptides were then precipitated and washed in cold ether, dissolved in distilled deionized water, desalted on a G-10 column (0.05% trifluoroacetic acid in water) and purified by reverse phase HPLC. Peptide purity and identity was confirmed by matrix-assisted laser desorption/ionization or electrospray ionization mass spectrometry.

III. Fluorescent labeling

The N-terminus of $D_{(142\text{-}154)}$–α–α was labeled with 5-((γ-glutamylaminoethyl) amino)naphthalene-1-sulfonic acid using the reagent 5-((2-(t-BOC)-γ-glutamylaminoethyl)

amino)naphthalene-1-sulfonic acid (Molecular Probes) during synthesis to generate edans-D(142-154)–α–α. Peptide purity and identity was confirmed by matrix-assisted laser desorption/ionization or electrospray ionization mass spectrometry.

IV. Circular dichroism spectroscopy

Circular dichroism spectra were recorded on an Aviv Circular Dichroism Spectrometer model 62DS at 25°C in a 1 mm quartz cuvette. Spectra were obtained from 190 to 260 nm (0.5 cm path length, 0.5 nm steps and 1 nm bandwidth) on samples containing 45 to 55 μM peptide in deionized and distilled water or 10 mM NaH_2PO_4, 120 mM NaCl, pH 7.

V. Assessing Cellular Proliferation using the XTT assay

Cells in the logarithmic phase of the growth cycle were washed two times in 137 mM NaCl, 2.7 mM KCl, 8.1 mM Na_2HPO_4, 1.5 mM KH_2PO_4, pH 7.4 (PBS). They were resuspended in culture media (as described above) without 2-mercaptoethanol. Two thousand cells were transferred to 96-well flat bottom plates and incubated with increasing amounts of cytokine needed for growth in a total volume of 100 μl. After incubation for 48 h at 37°C and 5% CO_2, sodium 3, 3'-{1-[(phenylamino) carbonyl]-3, 4-tetrazolium}- bis (4-methoxy-6-nitro) benzene sulfonic acid hydrate (XTT) (Diagnostic Chemicals Limited) and phenazine methosulfate (Sigma) were added to a final concentration of 0.2 mg/ml and 25 μM, respectively (Roehm et al, 1991). After incubation for another 4 to 8 h at 37°C and 5% CO_2, absorbance measurements were taken at 450 nm using an ELISA microtiter plate reader. The absorbance of a microtitre well containing XTT, phenazine methosulfate and

culture media was used as the sample reference. Absorbance at 450 nm is proportional to the number of static or proliferating cells. Proliferation curves for each of the cell lines were determined by non-linear least squares fitting to equation 1 (Matthews et al., 1996), using the program KALEIDAGRAPH (Synergy Software, Reading, PA)

$$\text{absorbance} = \frac{\left(\text{absorbance}_{max} - \text{absorbance}_{min}\right)}{1 + \left(\frac{[\text{cytokine}]}{EC_{50}}\right)^{n}} + \text{absorbance}_{min} \qquad \text{(Equation 1)}$$

The EC_{50} is the concentration of cytokine needed to obtain a 50% growth response and n is the cooperativity parameter.

VI. Effect of Peptides on Cellular Proliferation using the XTT assay

Cells were washed two times in PBS and resuspended in culture media (as described above) without 2-mercaptoethanol. The media was supplemented with its essential growth factor at a concentration corresponding to the EC_{80} as determined using the cellular proliferation assay. Two thousand cells were transferred to 96-well flat bottom plates and incubated with increasing amounts of peptide ranging from 0 to 120 μM in a total volume of 100 μl. After plates were incubated for 48 h at 37°C and 5% CO_2, XTT and phenazine methosulfate were added to a final concentration of 0.2 mg/ml and 25 μM, respectively (Roehm et al., 1991). After incubation for another 4 to 8 h at 37°C and 5% CO_2, absorbance measurements were taken at 450 nm using an ELISA multititer plate reader. The absorbance of a microtiter well containing XTT, phenazine methosulfate and culture media was used as

the sample reference. IC_{50} values were determined by non-linear squares fitting to equation 2 (Matthews et al., 1996), using the program KALEIDAGRAPH.

$$\text{absorbance} = \frac{\left(\text{absorbance}_{max}\right)}{1 + \left(\frac{[EPO]}{IC_{50}}\right)^{n}} \qquad \text{(Equation 2)}$$

The IC_{50} is the concentration of peptide needed to inhibit 50% cell proliferation and n is the cooperativity parameter.

VII. Sedimentation equilibrium experiments

Sedimentation experiments were performed at 20°C on a Beckman XLI Analytical Ultracentrifuge using an AN50-Ti rotor and sapphire windows. The sedimentation equilibrium experiments using six-channel charcoal-Epon cells were performed at 45 000 rpm for 30 h to ensure that equilibrium was reached before absorbance measurements were taken. Two samples were analyzed simultaneously at 20°C. The first sample contained 55 μM of edans-D(142-154)–α–α, 10 mM NaH_2PO_4, 5 mM EDTA, pH 7. The second sample contained 55 μM of the extracellular domain of human EPOR (soluble EPOR) and 55 μM of edans-D(142-154)–α–α, 10 mM NaH_2PO_4, 5 mM EDTA, pH 7. Protein concentration gradients formed at equilibrium were determined by measuring absorbances at 290 nm and 340 nm as a function of radial position.

VIII. Viability of cells assessed by light microscope

BaF3 cells were washed two times in PBS and resuspended in RMPI complete media

at a concentration of 1 x 10^6 cells/ml. One aliquot of cells was incubated with 80 μM D(142-154)–α–α, and a second aliquot was left untreated. At various times, 12000 cells were removed from the mixture and incubated with trypan blue (to a final concentration of 10%). Cells were examined by an inverted light microscope (Nikon TMS) using an oil immersion (50x) objective. Photos were taken on a Nikon FX-35A camera using 100 ASA film.

VIII. Flow Cytometry

BaF3 cells were washed two times in PBS and resuspended in RPMI 1640 complete media at a concentration of 1 x 10^6 cells/ml. Two aliquots of cells were prepared. The first aliquot was incubated with 80 μM D(142-154)–α–α and the second left untreated. 1 x 10^5 cells from each aliquot were taken out at 0 min, 10 min, 30 min and 3 h 45 min, washed with PBS, resuspended in 50 μl PBS, and incubated with 2 μl of 7-AAD for 5 min. Samples were then analyzed on a FACscan Becton Dickinson flow cytometer using CELLQuest software. Ten thousand events were analyzed for each time point.

C. Results

I. Rationale

The monomeric cytokine, EPO, binds two EPO receptors on the surface of the cell resulting in the formation of EPOR dimers (Syed et al., 1998). Dimer formation initiates the EPO signaling pathway leading to growth and differentiation of red blood cell progenitors. The crystal structure of the human EPO-EPOR complex confirms that EPO is a helical bundle composed of 4 amphipathic helices and contains two distinct EPOR binding sites, Site 1 and Site 2 (Syed et al., 1998). Site 1 is composed primarily of the A helix, A–B linker, and the D helix; Site 2 is composed primarily of the A and C helices. However, mutagenesis studies indicate that residues, which make up Sites 1 and 2, do not contribute equally to bioactivity. Specifically, Lys45 of the A–B linker and Asn147, Arg150, and Gly151 of the D helix contribute most to the bioactivity of Site 1 (Wen et al., 1994; Elliott et al., 1997). Arg14 and Tyr15 of the A helix, and Ser100, Arg103, Ser104, and Leu108 of the C helix contribute most to bioactivity of Site 2. The crystal structure of the EPO-EPOR complex shows that residues 140 to 155 of the D helix comprise that part of site 1 that is the most contiguous in sequence (Syed et al., 1998). Similarly, the most continuous segment of site 2 is residues 96 to 110 of the C helix. Furthermore, these continuous regions of Sites 1 and 2 contain most of the residues that are critical for bioactivity (Wen et al., 1994; Elliott et al., 1997). Based on these studies, we hypothesized that a synthetic molecule containing either the C or D helical segments (but not both) will have the potential to bind EPOR, prevent dimer formation, and thus act as an EPOR antagonist.

However, synthesis of only the C or D helical segments will likely be devoid of

binding activity because isolated helical segments of natural proteins are usually unstructured (Epand and Scheraga, 1968; Taniuchi and Anfinsen, 1968). We have devised a method to display segments of amphipathic EPO helices while retaining its native helical structure. Our method exploits the amphipathic nature of cytokine helices (Bazan, 1990) and can be applied to all helical cytokines that employ helical segments for binding. Kamtekar et al. (1993) have generated a library of helical bundles in which the helical segments possess amphipathic character but otherwise have random sequences. Structural analysis of this library has revealed that many of these molecules possess stable helical structure but fluctuating tertiary structure, typical of molten globules (Kuwajima, 1989). We hypothesized that the added flexibility of molten globules can be exploited to generate helical molecules that bind cytokine receptors and function as antagonists. Specifically, by linking one amphipathic cytokine segment to a number of generic amphipathic helices, a molten helical bundle will be produced in which the helical structure of the cytokine segment is preserved, and thus, enhancing the potential for receptor-binding.

II. Peptide design

Since our ultimate objective is to produce a small molecule cytokine antagonist, it is important to minimize the size of the cytokine–helical bundle. The smallest helical bundle known to be stable is a 3-helix bundle (McKnight et al., 1996), and the smallest known amphipathic peptide that forms helical assembles is a peptide known as alpha 1 (Hill et al., 1990). We therefore selected the 3-helix bundle motif for our designed antagonists, and based the generic amphipathic helices in our design on the sequence of alpha 1. The general topology of our designed peptides is: cytokine helix - loop - generic helix - loop - generic

helix. We used 5 Gly residues for the loop sequence because of the inherent flexibility of this amino acid residue. The sequences of the cytokine helix segment were taken from various regions of the C and D helices of human EPO which contain biologically important residues, as discussed above. The specific sequences of EPO examined were: residues 96-108 and 98-110 from the C helix as well as residues 140-152, 142-154, 145-157, and 147-159 from the D helix. At the C-terminal end of each peptide, a Gly-Gly-Tyr sequence was added. The Tyr residue facilitates the measurement of peptide concentration by absorbance (Chakrabartty et al., 1993), and the Gly residues serve as a flexible linker that prevent potential steric clashes between the C-terminal Tyr and the rest of the helical bundle.

Table 1 lists the names and sequences of each peptide synthesized. The name of each peptide was derived from its design components. For example, the C(96-108)–α–α peptide is made up of residues 96 to 108 from the C helix of human EPO linked to two generic amphipathic helices (α), with 5 Gly residues separating each helix.

A 3-helix bundle composed of three generic amphipathic helices, α–α–α, and 13-residue peptides corresponding to the EPO segments used, were synthesized as controls. The 13-residue peptides were also named according to their design elements, D(142-154) and D(145-157).

III. Secondary Structure of Designed Peptides

The secondary structures of the designed peptides were determined by circular dichroism spectroscopy. Figure 10 shows the circular dichroism spectra of all EPO-based

Table 1

Sequences of Erythropoietin-based Peptides

The residues in bold have been identified by mutagenesis to be biologically important. Underlined residues identify the sites that were mutated.

Peptide	Sequences
α–α–α	ELIKKILEELKGGGGGELIKKILEELKGGGGGELIKKILEELKGGY
D(142-154)	F**R**VYS**N**FL**RGK**LK
D(145-157)	YS**N**FL**RGK**LKLYT
C(96-108)–α–α	D**K**AV**S**GL**RS**LTT**L**GGGGGELIKKILEELKGGGGGELIKKILEELKGGY
C(98-110)–α–α	AV**S**GL**RS**LTT**L**LRGGGGGELIKKILEELKGGGGGELIKKILEELKGGY
D(140-152)–α–α	**K**LF**R**VYS**N**FL**RGK**GGGGGELIKKILEELKGGGGGELIKKILEELKGGY
D(142-154)–α–α	F**R**VYS**N**FL**RGK**LKGGGGGELIKKILEELKGGGGGELIKKILEELKGGY
D(145-157)–α–α	YS**N**FL**RGK**LKLYTGGGGGELIKKILEELKGGGGGELIKKILEELKGGY
D(147-159)–α–α	**N**FL**RGK**LKLYTGEGGGGGELIKKILEELKGGGGGELIKKILEELKGGY
N147K/R150E/G151A	F**R**VYS**K**FL**EA**KLKGGGGGELIKKILEELKGGGGGELIKKILEELKGGY

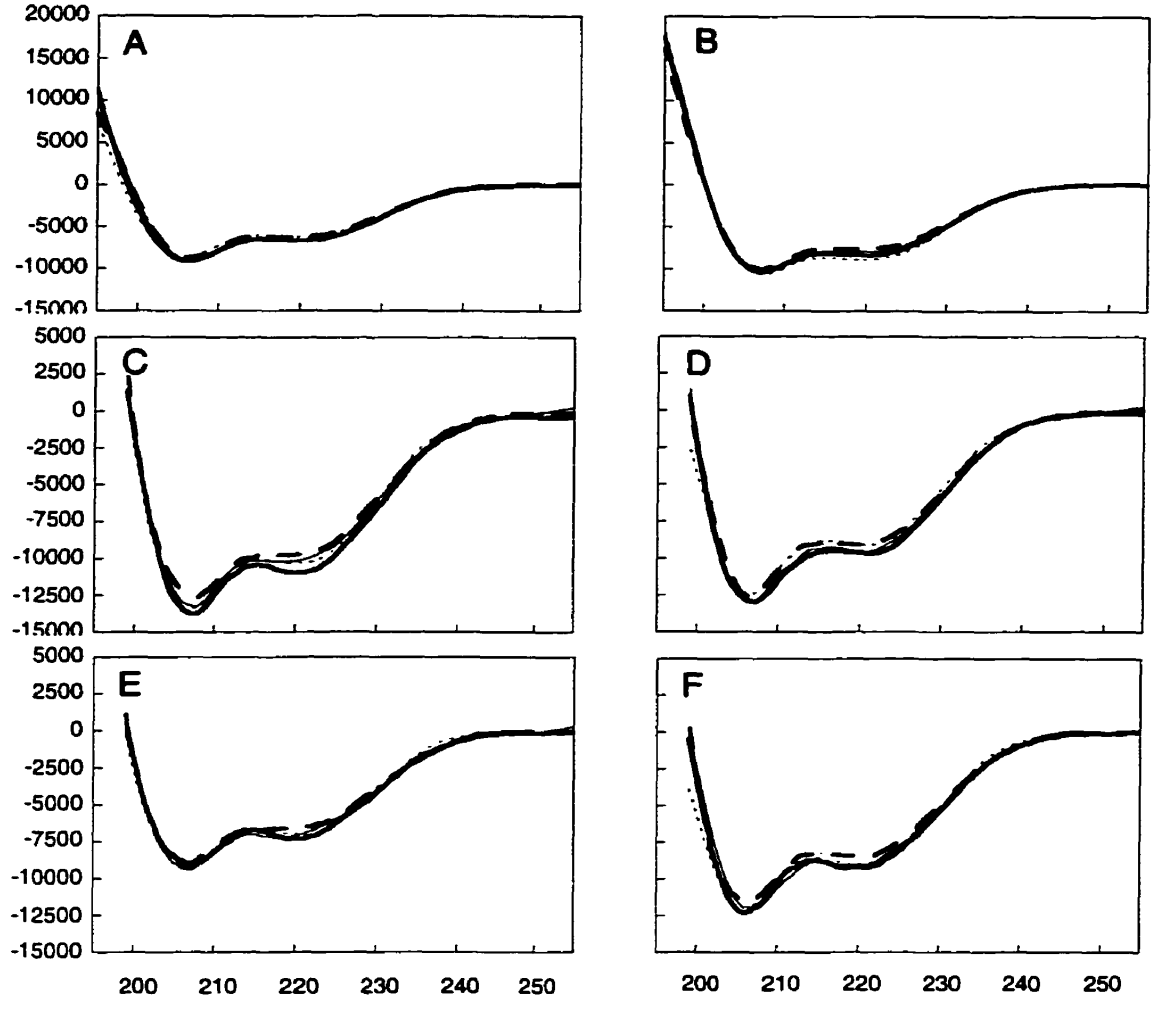

Fig. 10 Circular dichroism spectra of EPO-based peptides at various temperatures

The circular dichroism spectra of EPO-based peptides were assessed at 4, 25, 37 and 45°C. At all temperatures, each spectrum is characteristic of an α-helical structure with minima at 208 nm and 222 nm (dotted line, 4°C; thick line, 25°C; thin line, 37°C; dashed line, 45°C) (A, C (96-108)–α–α in 10 mM NaH_2PO_4 and 120 mM NaCl, pH 7; B, C(98-110)–α–α in 10 mM NaH_2PO_4 and 120 mM NaCl, pH 7; C, D(140-152)–α–α in distilled and deionized water; D, D(142-154)–α–α in distilled and deionized water; E, D(145-157)–α–α in distilled and deionized water; F, D(147-159)–α–α in distilled and deionized water).

peptides over a range of temperature from 4 to 45°C. All spectra are characteristic of α-helical structure with minima at 208 nm and 222 nm and do not change significantly with temperature. Urea denaturation experiments of α–α–α, C(96-108)–α–α and C(98-110)–α–α were also performed, and all 3 peptides displayed cooperative unfolding (data not shown). Cooperative urea denaturation and gradual non-cooperative thermal denaturation are hallmarks of molten globules (Bryson et al., 1995). Therefore, the EPO-based peptides appear to have molten globule characteristics.

Not surprisingly, the 13-residue control peptides, D(142-154) and D(145-157), were not helical (data not shown). This is consistent with isolate segments of helical proteins being unstable when removed from the original protein (Epand and Scheraga, 1968; Taniuchi and Anfinsen, 1968).

These results demonstrate that we are able to graft a helical segment of EPO onto a helical bundle scaffold to produce a 3-helix bundle with molten globule properties.

IV. Inhibition of Cell Proliferation by Erythropoietin-based Peptides

We examined the ability of the designed peptides to inhibit proliferation of a panel of 10 distinct cell lines derived from myeloid and lymphoid origin. For survival and proliferation, all the cell lines are factor-dependent and require the addition of exogenous cytokines, namely EPO, IL-2, IL-3 or IL-6. In addition, a fibroblast cell line, GP+E, that does not require exogenous cytokine was also included in this panel. The effect of the peptides on proliferation of these cells was assessed by the XTT assay. The principle of this

colorimetric assay is that XTT, a tetrazolium reagent, is reduced to a highly coloured, water soluble formazan product by dehydrogenase enzymes in viable cells.

Among the peptides studied, D(142-154)–α–α was the greatest inhibitor of cell proliferation. It inhibited proliferation of all cell lines examined, with IC_{50} values ranging between 5 and 26 μM (Table 2). The rank order potencies of the peptides containing cytokine segments from the D helix of EPO was, in decreasing order, D(142-154)–α–α, D(140-152)–α–α, D(145-157)–α–α, and D(147-159)–α–α. The D(147-159)–α–α was active in only half of the cell lines. The other peptides containing D helix segments had intermediate potency. The concentration-dependent decrease in proliferation was sigmoidal in shape (Fig. 11).

Of the two peptides derived from the C helix of EPO, the C(98-110)–α–α inhibited proliferation of 6 out of the 10 cell lines, with IC_{50} values ranging between 27 and 120 μM. The other C-helix peptide, C(96-108)–α–α, was not active in any of the cell lines tested.

The control peptides, α–α–α, D(142-154) and D(145-157), did not inhibit proliferation of any cell lines examined.

A mutant of D(142-154)–α–α was also synthesized. In this mutant (N147K/R150E/G151A), Asn147, Arg150 and Gly151 of D(142-154)–α–α were mutated to Lys, Glu and Ala, respectively. These substitutions were chosen because they showed the

Table 2

IC_{50} (μM) of various cell lines treated with erythropoietin-based peptides

All cell lines except for GP+E are hematopoietic in origin, and were cultured in the presence of exogenous cytokines, which are indicated in parentheses. GP+E are fibroblasts that do not require addition of exogenous cytokines. IC_{50} values are the concentrations (μM) of peptide required for 50 percent inhibition of cell proliferation.

	Cell Lines									
Peptide	UT7-EPO[a] (EPO)	HCD-57 (EPO)	BaF3-EPOR (EPO)	BaF3 (IL-3)	DA3 (IL-3)	FDCP (IL-3)	CTLL (IL-2)	CTLL-EPOR (IL-2)	B9 (IL-6)	GP+E
D(142-154)–α–α	26	9.6	19	13	9.9	12	5.1	4.8	19	28
D(140-152)–α–α	73	7.9	30	30	---[b]	---	---	---	35	---
D(145-157)–α–α	inactive	16	33	62	29	25	17	13	inactive	---
D(147-159)–α–α	inactive	22	69	inactive	inactive	inactive	50	50	inactive	---
C(98-110)–α–α	120	44	48	inactive	inactive	100	27	28	inactive	inactive
C(96-108)–α–α	inactive	inactive	---	inactive	inactive	inactive	inactive	inactive	inactive	inactive
α–α–α	inactive	inactive	inactive	inactive	inactive	inactive	inactive	inactive	inactive	inactive
D(142-154)	inactive	inactive	inactive	---	inactive	inactive	inactive	inactive	inactive	inactive
D(145-157)	inactive	inactive	---	---	inactive	inactive	inactive	inactive	inactive	inactive
N147K/R150E/G151A	inactive	inactive	48	inactive	---	58	---	---	---	---

[a]UT7-EPO cells are a human cell line; all other cell lines are of murine origin.

[b]---, Not tested.

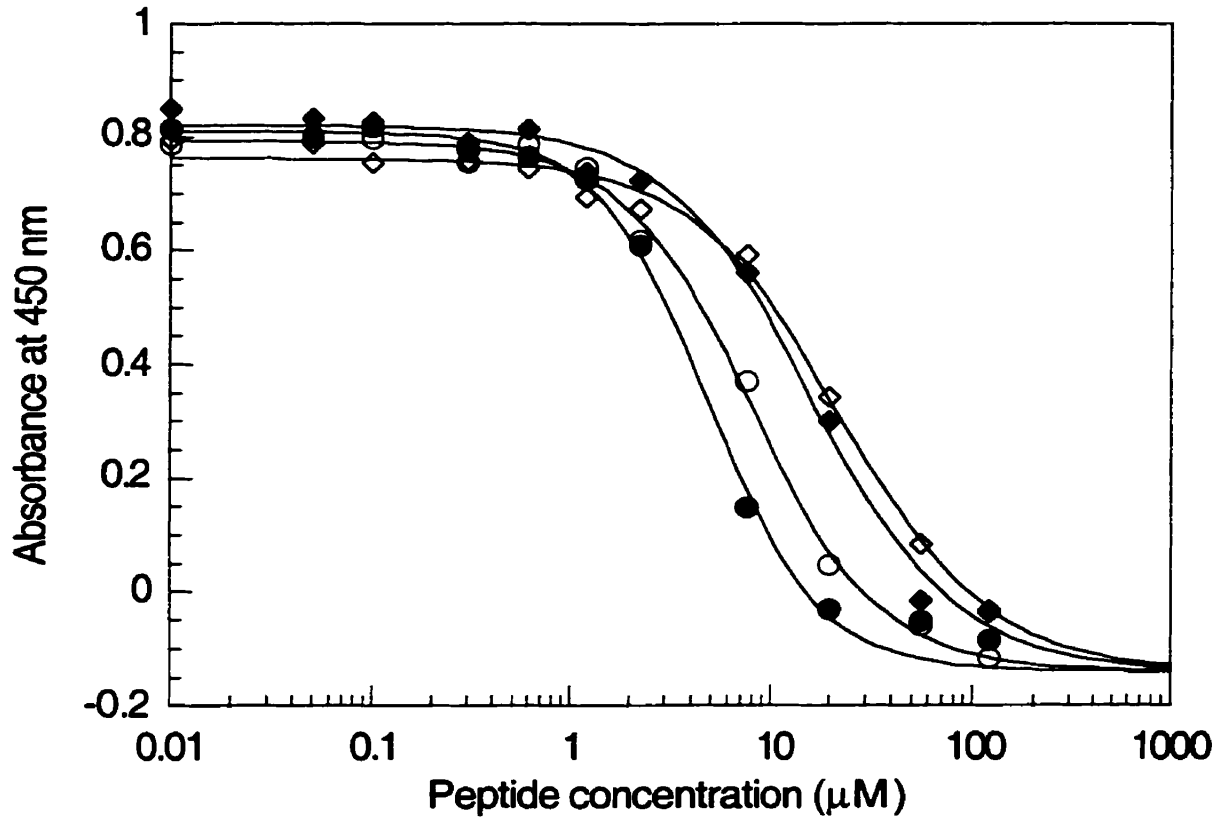

Fig. 11 Effect of concentration of EPO-based peptides on proliferation of EPO-dependent cells, HCD-57

Cells (2500 per well) were incubated with increasing concentrations of peptide in Iscove's complete media supplemented with EPO (0.375 units/ml). Cell proliferation was measured with the XTT assay after 48 h. (O, D(140-152)–α–α; ●, D(142-154)–α–α; ◆, D(145-157)–α–α; ◊, D(147-159)–α–α)

largest reduction in EPO bioactivity (Elliott et al., 1997; Syed et al., 1998). The mutant was inactive in 3 of the 5 cell lines tested. In the 2 cell lines where the mutant was active, the IC_{50} values were 2.5- and 4.8-fold higher than the respective IC_{50} values for D(142-154)–α–α.

In summary, D(142-154)–α–α was found to be the most potent inhibitor of cell proliferation. This peptide inhibited proliferation of cells that required the addition of EPO for growth. Surprisingly, this peptide also exhibited similar effects on hematopoietic cells that required the addition of IL-2, IL-3 or IL-6 for growth, as well as on fibroblasts that did not require exogenous cytokines. Neither the peptide that represented the isolated cytokine segment, D(142-154), nor the peptide that represented the generic amphipathic helices, α–α–α, inhibited cellular proliferation in all cell lines examined.

V. Interdependence of EPO and D(142-154)–α–α Activities

The observation that D(142-154)–α–α inhibited proliferation of cells that did not express the EPO receptor raised the possibility that the growth inhibitory activity was unrelated to EPO signaling. To explore this possibility further, the bioactivity of EPO was measured with varying concentrations of peptide, and the bioactivity of the peptide was measured with varying concentrations of EPO. The EC_{50} values of EPO-induced proliferation of HCD-57 cells were unchanged at 0.02 units/ml when the D(142-154)–α–α concentration was raised from 0 to 50 μM (Fig. 12). Similarly, in the reciprocal experiment, the IC_{50} values of D(142-154)–α–α-induced inhibition of cell proliferation were maintained between 30 and 80 μM when the concentrations of EPO was increased from 0.005 to 2

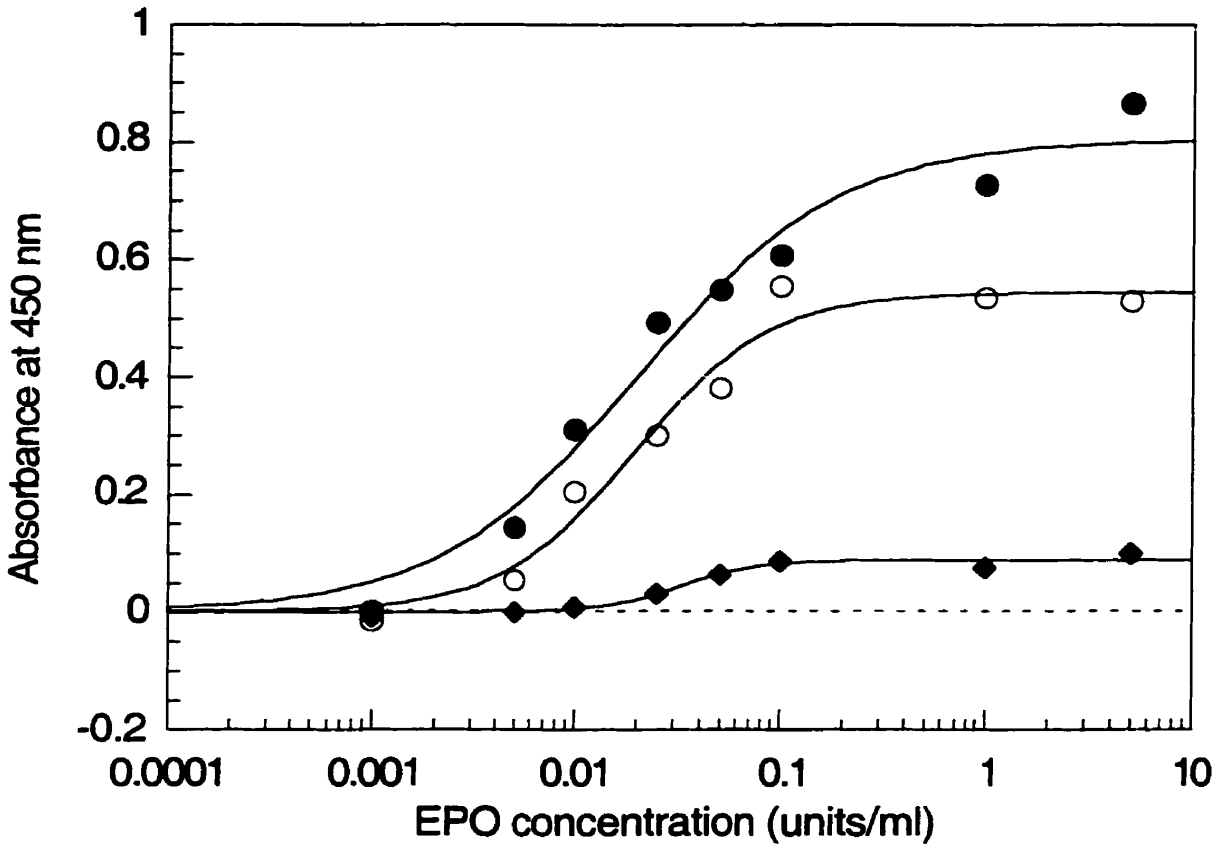

Fig. 12 Effect of concentration of EPO on proliferation of EPO-dependent HCD-57 cells, in the presence of varying concentrations of D(142-154)–α–α

Cells (2000 per well) were incubated with 0, 25 and 50 μM of peptide and increasing amounts of EPO for 48 h. Cell proliferation was assessed by XTT assay. (●, 0 μM D(142-154)–α–α; O , 25 μM D(142-154)–α–α; ◆, 50 μM D(142-154)–α–α; dotted line, cells incubated without EPO)

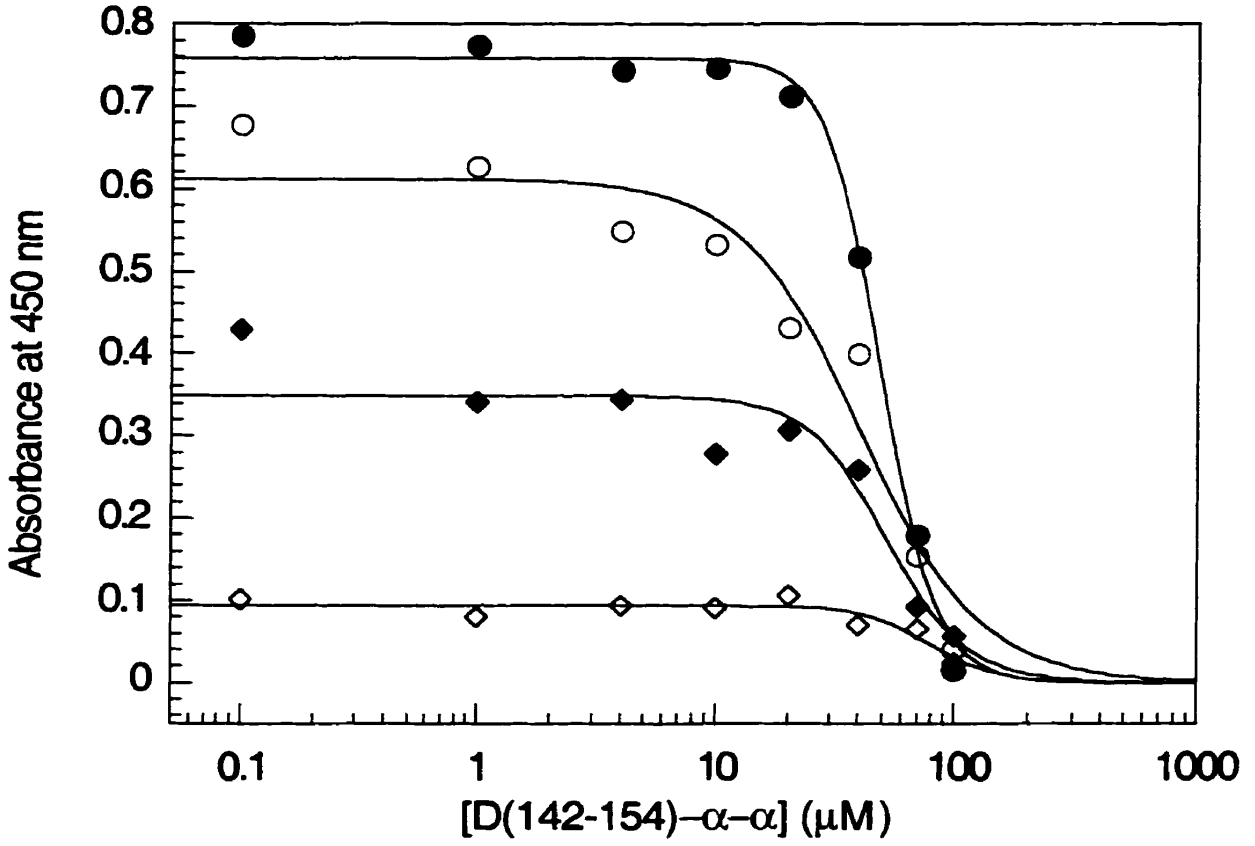

Fig. 13 Effect of concentration of D(142-154)–α–α on proliferation of EPO-dependent HCD-57 cells, in the presence of varying concentrations of EPO

Cells (2000 per well) were incubated with 0.005, 0.015, 0.05 and 0.2 units/ml of EPO and increasing amounts of peptide for 48 h. Cell proliferation was assessed by XTT assay. (●, 0.2 units/ml EPO; O, 0.05 units/ml EPO; ◆, 0.015 units/ml EPO; ◊, 0.005 units/ml EPO)

units/ml (Fig. 13). These data indicate that the peptide activity and EPO activity are not interdependent.

VI. Binding of D(142-154)–α–α Peptide to Soluble EPOR

Demonstrating that D(142-154)–α–α functioned independently of EPO raised the question of whether D(142-154)–α–α was capable of binding EPOR. To investigate this further, we examined the interaction between D(142-154)–α–α and soluble EPOR by analytical ultracentrifugation. Previous ultracentrifugation studies show that mixtures of EPO and soluble EPOR form EPO-EPOR complexes (Philo et al, 1996). At lower concentrations, it was found that a single EPO molecule bound a single EPOR molecule to form a 1:1 complex; conversely, at higher concentrations, a mixture of 1:1 and 1:2 EPO:EPOR complexes was seen. To investigate the likelihood that D(142-154)–α–α forms a complex with soluble EPOR, we also utilized analytical ultracentrifugation; however, we employed modifications to increase the sensitivity of detecting complexes of D(142-154)–α–α and soluble EPOR, which may not be significantly populated. Specifically, we used a form D(142-154)–α–α which was labeled with a chromophore edans to produce edans-D(142-154)–α–α. This chromophore has an absorbance maximum at 340 nm and allows specific detection of the peptide in the presence of other proteins that do not absorb light of 340 nm. Prolonged centrifugation of a solution of edans-D(142-154)–α–α at high speeds establishes an equilibrium in which the peptide is depleted from the meniscus and forms a concentration gradient down the centrifugation cell. The concentration gradient can be determined by measuring the absorbance (at 340 nm) at different positions along the centrifugation cell, and

its shape is dependent on the molecular weight of the peptide. If soluble EPOR is also present in the centrifugation cell and forms complexes with D(142-154)–α–α, then the concentration gradient of edans-D(142-154)–α–α will change due to the increase in its apparent molecular weight.

The edans-D(142-154)–α–α used in the experiments possessed bioactivity similar to the unlabeled D(142-154)–α–α in HCD-57 cells (data not shown). The soluble EPOR used in the experiments caused a dose-dependent inhibition of proliferation of HCD-57 and BaF3 cells grown in the presence of EPO; the IC_{50} value was 3 nM (data not shown).

Two samples were used for analytical ultracentrifugation, one with only 55 μM edans-D(142-54)–α–α and the other with 55 μM edans-D(142-54)–α–α and 55 μM soluble EPOR. After equilibrium was reached, the concentration gradients were determined by absorbance measurements at 340 nm and are shown in Fig. 14a. The concentration gradients of both samples were superimposable suggesting that complexes between edans-D(142-154)–α–α and soluble EPOR were not being formed. To ensure that the soluble EPOR was present and had not degraded or aggregated during centrifugation, concentration gradients were also determined by measuring absorbance at 290 nm as a function of different positions along the centrifugation cell (i.e. radial position). At this wavelength, both the edans chromophore of edans-D(142-154)–α–α and Trp residues of the soluble EPOR absorb light. Hence, concentration gradients determined at 290 nm should differ between the two samples. This indeed was the case (Fig. 14b), thus it appears that the soluble EPOR had not aggregated or degraded. In summary, the analytical ultracentrifugation experiments provide significant

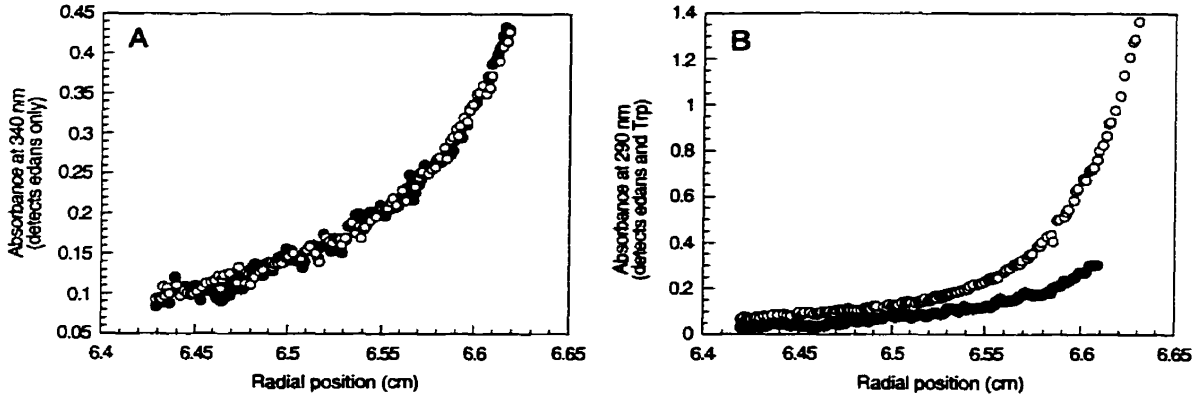

Fig. 14 Sedimentation equilibrium analysis of edans-D(142-154)–α–α in the presence and absence of soluble human EPOR

Two samples were analyzed. The first sample contained 55 μM edans-D(142-154)–α–α and the second sample contained 55 μM of soluble EPOR and 55 μM edans-D(142-154)–α–α. Samples were centrifuged using a Beckman XLI analytical ultracentrifuge and an AN50Ti rotor. Centrifugation conditions: 45000 rpm, 10 mM NaH_2PO_4, 5 mM EDTA, pH 7, 20°C. (A) Concentration gradients were determined by monitoring the absorbance at 340 nm. At this wavelength, only the edans moiety contributes to the absorbance signal. (B) Concentration gradients were determined by monitoring the absorbance at 290 nm. At this wavelength, both edans-D(142-154)–α–α and Trp residues of soluble EPOR contribute to the absorbance signal (●, edans-D(142-154)–α–α only; O, edans-D(142-154)–α–α and soluble EPOR)

evidence that D(142-154)–α–α does not interact with soluble EPOR. Thus, the growth-inhibitory activity of the EPO-based peptides appears to act through a pathway unrelated to EPO signaling.

VII. Kinetics of the inhibition of proliferation by EPO-based peptides

To investigate the mechanism by which the EPO-based peptides inhibit proliferation, the kinetics of inhibition were examined using two assays for cell viability using BaF3 cells. The first assay involved monitoring uptake of the dye, trypan blue, over a period of 3h 45 min hours after the addition of 80 μM D(142-154)–α–α. Fig. 15 shows that although cells incubated with inhibitory peptides were undergoing cell death by as early as 30 min (Fig. 15e), resting cells did not stain positive even after 3h 45 min (Fig. 15c). These data indicate that the plasma membranes of these cells are rapidly compromised after addition of peptide.

The second assay quantified the rate at which membrane integrity was compromised. A flow cytometer was used to monitor the relative number of BaF3 cells that took up 7-AAD, a fluorescent DNA intercalator (Schmid et al., 1992). The uptake rate was rapid and exponential (Fig. 16). Within 10 min, 25% of the cells took up 7-AAD, uptake reached 50% and 90% by 30 min and 3 h 45 min, respectively. Untreated cells did not show significant levels of 7-AAD uptake.

The uptake of trypan blue and 7-AAD clearly show that the peptide is compromising the integrity of the plasma membrane of cells at a rapid rate. This membrane perturbation phenomenon may represent the mechanism by which these peptides inhibit proliferation of the diverse cell types present in our panel (Table 2).

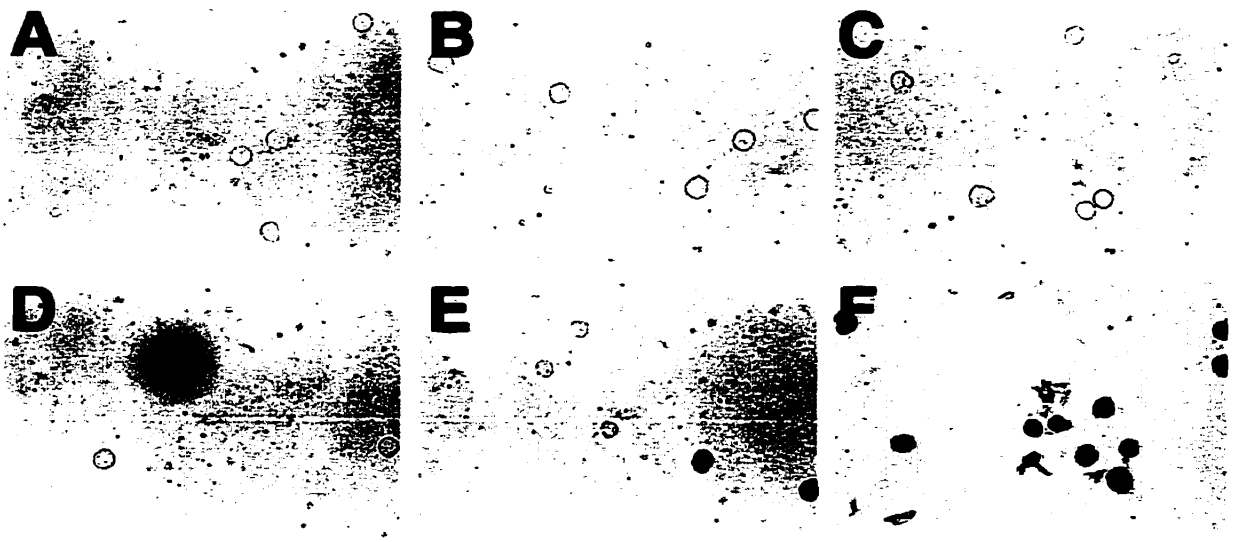

Fig. 15 Uptake of trypan blue by BaF3 cells incubated with 80 μM D(142-154)–α–α

BaF3 cells in RMPI complete media were treated in the presence and absence of peptide. At various time points, cells were assessed for viability using 10% trypan blue and observed under a light microscope (50x). (A) Untreated BaF3 cells at 0 min (B) Untreated BaF3 cells at 30 min (C) Untreated BaF3 cells at 3 h 45 min. (D) BaF3 cells + peptide at 0 min (E) BaF3 cells + peptide at 30 min (F) BaF3 cells + peptide at 3 h 45 min.

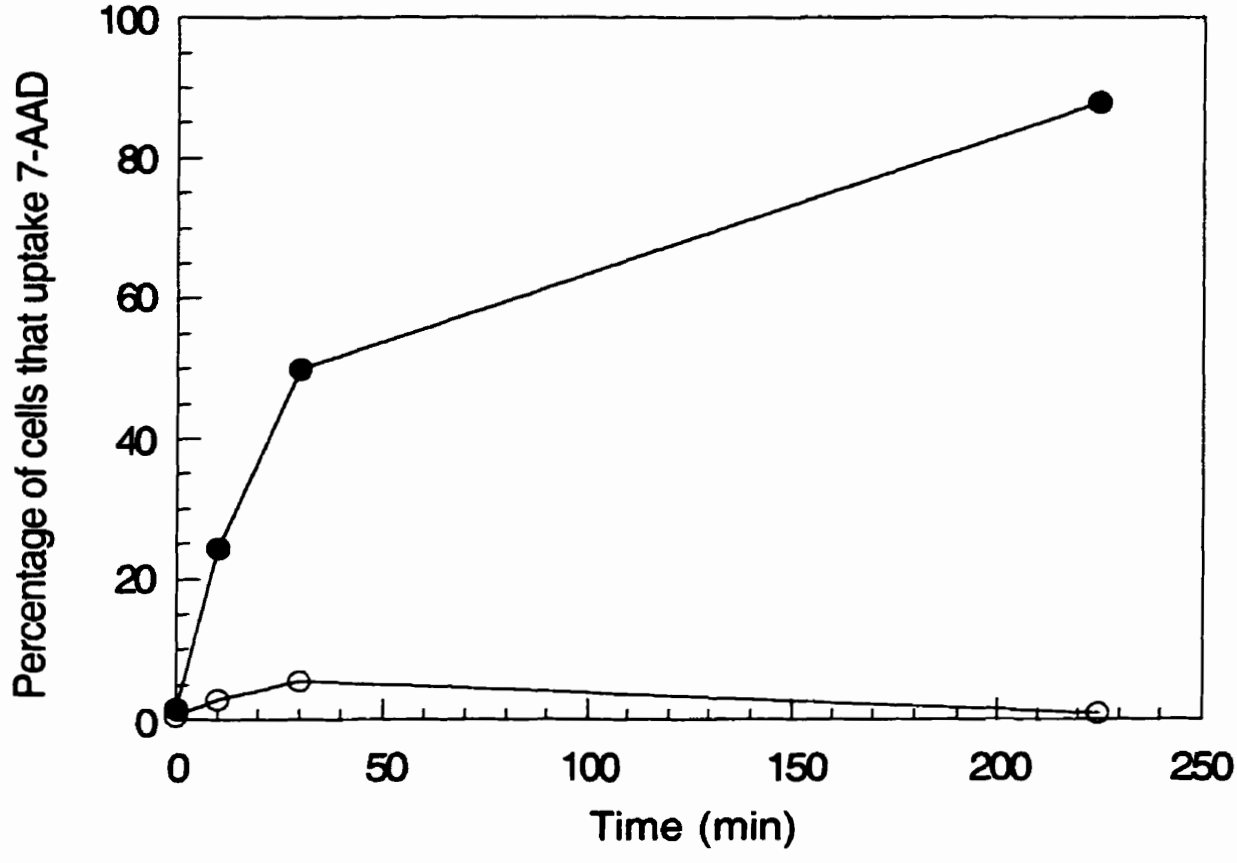

Fig. 16 Uptake of 7-AAD in BaF3 cells incubated with 80 μM D(142-154)–α–α

One hundred thousand cells in RPMI complete media were incubated in the presence and absence of peptide. Flow cytometry analysis was used to monitor uptake of 7-AAD at various time points. Each time point encompassed 10000 events. (●, 80 μM D(142-154)–α–α; O, 0 μM D(142-154)–α–α)

D. Discussion

I. Development of a versatile scaffold for presentation of amphipathic helices.

In the present study, we have grafted various 13-residue segments derived from amphipathic helical regions of EPO onto a scaffold to produce 3-helix bundles. The EPO segments varied vastly in their sequences, and were unstructured in isolation; however, helical structure was induced upon assembly of the helical bundles. These bundles displayed cooperative urea-induced unfolding and non-cooperative thermal denaturation, suggesting the presence of molten globule structures.

This method can be used to display any short amphipathic peptide segment in a helical conformation. Potential applications for this method include constraining peptide segments in helical conformation during phage display, generation of conformation-specific antibodies, and presentation of helical binding epitopes.

Recent studies have shown that leucine-zippers can also be used to present helical sequences in a stable structure (Butcher et al., 1997; Domingues et al., 1999). While leucine-zipper scaffolds have the advantage of being more native-like in structure and thus, more resistant to degradation, they require that the helical segment be ~30 residues in length. Our designed molecules have the advantage of being able to present shorter helical segments that are more representative of helices in natural proteins.

II. Interactions of designed EPO-based peptides with EPOR.

One of the aims of this work was to use our method to design antagonists of helical

cytokines, employing EPO as a model cytokine. Segments of EPO known to be important for bioactivity were grafted onto the generic scaffold forming helical bundles with molten globule characteristics. We reasoned that these EPO-based helical bundles would bind EPOR and inhibit homodimerization of the receptor. Furthermore, the added flexibility of the molten globule nature of these helical bundles was predicted to facilitate binding by allowing for adjustments in structure to optimize interactions with the receptor. While the structural features of the EPO-based molecules were successfully designed, these molecules did not bind the EPOR. Analytical ultracentrifugation behavior of the EPO-based peptide was unaffected by the presence of soluble EPOR, indicating the peptide does not interact with the receptor.

To investigate whether the EPO-based peptides interact with the EPOR on the surface of cells, we examined whether there was interdependence between the activities of the EPO-based peptides and EPO. Specifically, we determined if the activity of the peptides were dependent on the concentration of EPO and conversely, if EPO-activity was dependent on the concentration of the peptides. If the molecules were binding to EPOR, the EC_{50} value of EPO-induced proliferation would increase with increasing concentration of D(142-154)–α–α. Similarly, the IC_{50} value of D(142-154)–α–α would increase with increasing concentrations of EPO. We observed that neither the EC_{50} value of EPO nor the IC_{50} value of D(142-154)–α–α was affected by changes in the concentration of the peptide and cytokine, respectively. Thus, it appears that the EPO-based peptides do not bind EPOR on the surface of cells.

The above observations show that the regions of EPO selected for presentation do not

provide sufficient binding energy to form a stable complex with EPOR. Because the residues that make up the functional epitopes, Site 1 and 2 of EPO, are not contiguous in sequence, it is possible that some or all of the noncontiguous regions are needed to obtain stable binding. Another possibility is that the helical scaffold causes steric interference between the EPO segment and the EPOR.

III. Cytotoxic activity of EPO-based peptides.

While the EPO-based peptides did not bind the receptor, they did have a potent cytotoxic activity against a wide spectrum of cell lines. The peptide with the greatest activity (D(142-154)–α–α) contained a cytokine segment that corresponds to residues 142-154 of the D helix of EPO. Peptides containing cytokine segments that were shifted 2 residues closer to the N-terminus of EPO and 3 or 5 residues closer to the C-terminus of EPO exhibited significantly lower activity or were inactive. Therefore, the cytotoxic activity appeared to have a critical sequence-dependence. However, the C(98-110)–α–α, which has a significantly different sequence from the peptides containing D helix cytokine segments, also possessed cytotoxic activity. Consequently, the sequence motif that is responsible for the cytotoxic activity may reside in a subset of residues. Alignment of the cytokine segments of C(98-110)–α–α, D(140-152)–α–α, and D(142-154)–α–α reveals a consensus pattern of RXXXXLR, where X is any amino acid. The i, i+6 spacing of the two Arg residues of the consensus sequence would place them on the same side of the helix. This consensus sequence may be responsible for the cytotoxic activity.

Alternatively, the cytotoxic activity of the designed peptides may arise from a

physico-chemical characteristic of the sequence of the cytokine segment, rather than from the sequence itself. We compared three physico-chemical characteristics of the cytokine segments with their respective cytotoxic activities. The characteristics were: the hydrophobic moment, which is a measure of helical amphiphilicity (Eisenberg et al., 1982), hydrophobicity, and net charge. The hydrophobic moments and hydrophobicities of the cytokine segments were determined using the methods of Eisenberg et al. (1984) and the net charge at neutral pH was calculated assuming that the Asp, Arg, Lys and Glu residues present in the cytokine segments were fully ionized. Correlation curves of the hydrophobic moments, hydrophobicities, and net charge against IC_{50} values revealed correlation coefficients of 0.759, 0.545 and 0.727, respectively. These relatively low coefficients suggest that the cytotoxic activity of the EPO-based peptide does not arise from these three physico-chemical characteristics.

The 13 residue peptides, D(142-154) and D(145-157), which correspond to residues 142-154 and 145-157 of EPO, respectively, were devoid of helical structure as well as cytotoxic activity. In order for these EPO segments to be cytotoxic, they needed to be grafted onto the helical scaffold. This demonstrates that the cytotoxic activity has specific requirements for both sequence and secondary structure.

IV. Mechanism of cytotoxic activity of EPO-based peptides.

The cytotoxic activity of the EPO-based peptides may be mediated through either necrotic or apoptotic mechanisms. Our data suggests that the peptides induce necrosis. A key distinction between the two mechanisms of cell death is that membrane damage is an

early event in necrosis and a late event in apoptosis. We have shown that BaF3 cells uptake the dye, 7-AAD, as early as 10 min after addition of D(142-154)–α–α, indicating that this peptide causes a rapid breakdown of membrane integrity. This conclusion is also supported by the results of trypan blue staining in which uptake of trypan blue was detected as early as 30 min. In summary, the rapid disruption of the plasma membrane by the EPO-based peptides suggests a necrotic mechanism.

V. Comparison of EPO-based peptides with other cytotoxic α-helical amphipathic peptides.

Interaction of natural and model amphipathic α-helical peptides with biological membranes have been studied in a number of different systems (Epand et al., 1995). Membrane active amphipathic helices are generally 18-25 residues in length and they interact with membranes by either lying along the membrane surface or penetrating into the bilayer. While surface association can disrupt the membrane through increasing the intrinsic curvature strain of bilayers, penetration of the bilayer induces membrane disruption through pore formation (Epand et al., 1995). Many membrane active peptides also exhibit cytotoxic activity (Agawa et al., 1991; Blondelle and Houghten, 1992). Interestingly, while the membrane activity is optimal for peptide lengths between 18-25 residues, the cytotoxic activity is optimal for lengths between 11-17 residues (Agawa et al., 1991; Blondelle and Houghten, 1992). One mechanism of cytotoxicity proposed for the short peptides which cannot span the membrane bilayer is that they form head-to-tail dimers of α-helices which assemble into ion channels (Anzai et al., 1991). The cytokine segments of our EPO-based peptides have a similar net positive charge, amphipathic character and length as the basic

amphipathic α-helical model peptides studied previously (Agawa et al., 1991; Blondelle and Houghten, 1992). This raises the intriguing possibility that the EPO-based peptides exhibit their cytotoxic activity by either disrupting the plasma membrane through surface association or by forming head-to-tail dimeric ion channels which destroy cellular osmotic homeostasis.

Chapter 3: Redesigning an EPO antagonist using a coiled coil scaffold

In the present study, we have examined a general method for designing antagonists of helical cytokines. This method involved grafting short amphipathic segments of a cytokine onto a helical scaffold to produce a 3-helix bundle. The specific goal of this work was to design an antagonist to bind the extracellular domain of a helical cytokine receptor. The designed molecule would bind one receptor and inhibit the native cytokine from oligomerizing the required number of receptors needed to initiate intracellular signaling events. EPO was chosen as our target cytokine. It was found that short amphipathic segments of EPO could retain its native helical structure when grafted onto a helical scaffold to produce a 3-helix bundle. However, the designed EPO-based peptides did not bind EPOR. Several factors may have contributed to this outcome: (1) the flexibility of the molecule due to its molten globule nature, (2) the relatively small segments of EPO chosen for presentation, and (3) the possible steric hindrance caused by the scaffold helices.

The designed EPO-based peptides were found to be molten globules. The hallmark of molten globules is that they posses defined secondary structure but lack unique or conformationally specific tertiary structure. The flexibility associated with the fluctuating tertiary structure of the molten globule was thought to be advantageous to our design method, as it was believed to facilitate binding by allowing for adjustments of the peptide structure to optimize interactions with the receptor. Our results, however, indicated that this flexibility did not promote binding. The loss of conformational entropy upon binding a molten globule is much greater than that of binding a native protein and may have prevented the EPO-based

peptides from binding the receptor. This suggests that a specific tertiary structure, like that of a native protein, may be needed to acquire specific binding activity. Aside from the molten globule characteristics of the EPO-based peptides, the length of the EPO sequences used could have also contributed to the inability of the peptides to bind EPOR. Binding of the peptides to EPOR would occur through interactions with the residues in the EPO segment of the 3-helix bundle. The EPO segments chosen may have been too short to provide sufficient binding energy to form a stable complex with EPOR. Increasing the length of the segments used may help to overcome this limitation. Lastly, there is a small possibility that the scaffold helices (–α–α) were in some way interfering with the ability of the EPO segments to interact with the receptor. This would have inhibited the EPO-based designed peptides from binding the receptor.

In view of these above-mentioned problems associated with using a designed 3-helix bundle as the helical scaffold, an alternative strategy to designing antagonists might be to employ a "natural motif" (Butcher et al., 1997). This approach involves transferring the binding sites of a target protein onto an unrelated, pre-existing sequence template (a natural protein) to generate the desired binding functions. Using natural helical proteins as a scaffold avoids the problems associated with the molten globule. The leucine zipper is a natural motif that has been recently used as a scaffold for designing functional peptides and proteins (Butcher et al., 1997; Domingues et al., 1999). This motif adopts a two-stranded coiled coil fold and has been shown to have the ability to present helical sequences in a stable structure. Designed coiled coils, typically ~30 amino acids, exhibit characteristics of a native protein such as a well-packed hydrophobic core, cooperative unfolding and a unique tertiary

structure.

Using a coiled coil as a helical scaffold in designing an EPO antagonist offers several benefits as compared to the designed 3-helix bundle described in Chapter 2: First, the designed coiled coils would have a more native-like structure than the designed 3-helix bundle, which were molten globules. The loss of conformational entropy in binding a native-like protein would be less than the loss in conformational entropy in binding a molten globule. Second, the relatively long helices of a coiled coil (~30 residues) as compared to the length of the helices of the designed 3-helix bundle (13 residues), would allow the entire D helix of EPO (23 residues in length) (Syed et al., 1998) to be presented to the receptor. Increasing the length of the EPO segment could provide additional binding energy required to facilitate binding to the receptor. Third, any steric hindrance caused by the orientation of the scaffolding helices in the 3-helix bundle could be minimized by using a two-stranded coiled coil. Therefore, using a coiled coil as a helical scaffold in designing an EPO antagonist may overcome the weaknesses associated with using the designed 3-helix bundle.

A. A Brief Overview of Coiled Coils

Coiled coil proteins are composed of a bundle of α-helices that are wound into a left-handed superhelix with approximately 3.5 residues per turn (Lupas, 1996). They have a characteristic heptad repeat in which seven residues, labeled *a* to *g*, recur in the sequence. Typically, the *a* and *d* positions are occupied by Leu, Ile and Val residues whose sidechains point toward the center of the superhelix, forming the helix interface (Mittl. et al., 2000).

Conversely, positions *b*, *c*, *e*, *f*, and *g* are occupied by hydrophilic amino acids that are solvent-exposed (Lupas, 1996). Coiled coil proteins consist of two to five intertwined α-helices and are frequently found in oligomeric proteins such as transcription factors and structural proteins (Beck and Brodsky, 1998). The number of helices in a coiled coil is determined by the packing of the core residues. Different amino acids in the *a* and *d* positions would have a different geometry with respect to the backbone as well as different sidechain preferences which would govern the formation of two-, three-, and four-stranded coiled coils (Lupas, 1996). The hydrophobicity of the core and its two flanking positions (*e* and *g* of the heptad repeat) also play a role in determining the number of strands in a coiled coil. For example, polar residues in the core favour dimer formation where they can still be solvated as compared to trimers and tetramers where the core is strongly shielded from the solvent (Lupas, 1996). The parallel or antiparallel orientation of the helices is primarily determined by polar and ionic interactions between residues flanking the hydrophobic core (*e* and *g* positions in the heptad repeat). Most interactions occur between residues in the *g* position of one heptad and the *e* position of the next heptad.

The basic region leucine zipper (bZIP) DNA-binding motif of the yeast transcription activator GCN4 is one of the most well characterized coiled coils. This 33-residue moiety is called a leucine zipper because it contains Leu residues at ~80 % of the *d* positions in the heptad repeat (Harbury et al., 1993). The crystal structure of the GCN4 leucine zipper was solved in 1991 (O'Shea et al., 1991) and was found to be a two-stranded, parallel coiled coil with an Asn16 in the hydrophobic face of each of its two helices. The Asn residue is a conserved residue found in a single *a* position of many bZIP proteins (Lupas, 1996). It forms

a hydrogen bond between its sidechain and the sidechain of the other corresponding Asn in the hydrophobic dimer interface (O'Shea et al., 1991).

B. Redesigning an EPO antagonist using a GCN4 leucine zipper as a scaffold

The GCN4 leucine zipper, comprised of Chains A and B, has been chosen as the natural structural motif for redesigning an EPO antagonist. As described above, using a coiled coil as a scaffold to design a molecule with the desired binding function would involve transferring the binding residues in EPO onto the coiled coil fold of the GCN4 leucine zipper. The residues of choice are those involved in the Site 1 binding of EPO and are located on Helix D. Two crystal structures were used to generate a model of the EPO antagonist: EPO bound to two EPObp (PDB accession code: 1EER) and GCN4 (PDB accession code: 2ZTA). The program Swiss-PdbViewer was used to build a model in which the Site 1 interacting residues in Helix D of EPO were transferred to the B chain of GCN4 by superimposing the two structures. All GCN4 leucine zipper core residues (*a* and *d* positions) were unchanged to maintain the coiled coil fold. In addition, most of the residues that flank the core (*e* and *g* positions) were also kept the same as they play a role in the oligomeric state of a coiled coil. The remaining solvent-exposed residues in the GCN4 leucine zipper were mutated to mimic the corresponding face of Helix D of EPO.

Chain B of GCN4 was visually superimposed onto Helix D of EPO such that the positions of the buried residues of both helices were aligned. This manual alignment

revealed that residues 2-21 of the B chain of GCN4 could align with residues 138-157 of Helix D of EPO. The "Fit Selection (for selected molecules)" function of the Swiss-PdbViewer program was used to generate a structural alignment using the above-mentioned regions of both molecules. The "Improve Fit" function was then employed to generate a better structural alignment. This alignment is shown in Fig. 17 and maps residues 1-23 of the B chain of GCN4 onto residues 137-160 of Helix D of EPO. The sequence of GCN4 was then modified to resemble the solvent- exposed face of Helix D of EPO. In determining which residues to mutate, the following criteria were implemented: (1) all *a, d, e, and g* positions of the heptad repeat in GCN4 were unchanged because they are required for stability and specificity of the leucine zipper, (2) all positions in GCN4 corresponding to the Site 1 receptor-binding sites (Lys140, Arg143, Ser146, Asn147, Arg150, Gly151, Lys154 and Leu155 (Syed et al., 1998)) of EPO were mutated to the corresponding residues found in EPO, and (3) the remaining solvent-exposed residues in GCN4 (positions *b, c* and *f*) were mutated to the corresponding EPO residues. There were two exceptions to the these criteria: First, as an exception to criteria (1), Lys15 of GCN4, which is a *g* position amino acid in the heptad repeat, was mutated to Gly because it was aligned with one of the Site 1 receptor-binding sites of EPO (Gly 151). Second, as an exception to criteria (3), Asn21 of GCN4, which is a *f* position amino acid in the heptad repeat, was not mutated to Gly despite the fact that it aligned with Gly158 in EPO. A mutation of Asn21 to Gly would introduce a helix breaker (Chakrabartty and Baldwin, 1995) into the GCN4 sequence that would likely destabilize the coiled coil fold. To eliminate the sidechain of Asn without changing the overall structure of GCN4, Asn21 was mutated to Ala. An Ala substitution has been shown to have a high helix propensity (Chakrabartty and Baldwin, 1995) and is not likely to result

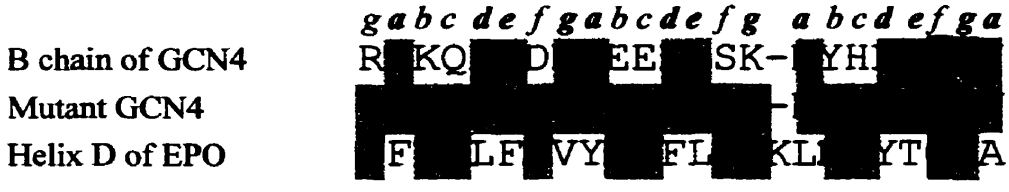

Fig. 17 Sequence alignment of GCN4, Mutant GCN4 and EPO

Sequence alignment of the B chain of GCN4 (residues 1-23), the B chain of Mutant GCN4 (residues 1-23) and Helix D of EPO (residues 137-160). The heptad repeat is labeled *a, b, c, d, e, f, g*. The *a, d, e,* and *g* positions of the heptad repeat are in bold type and are important for stability and specificity of the coiled coil. Shaded boxes indicate the residues that are in common. The Asn21 to Ala mutation is highlighted in green. Residues in Helix D of EPO that interact with EPOR at Site 1 (Syed et al., 1998) are in bold type. This figure was generated using Swiss-PdbViewer.

in large perturbations in the structure. The final step in designing the antagonist, referred to as Mutant GCN4, was to make identical changes in Chain A of the GCN4 leucine zipper.

C. Evaluation of the Model

A model of the EPO antagonist, Mutant GCN4, was built using the Swiss-PdbViewer software. Fig. 18 shows Chain B of Mutant GCN4 superimposed on Helix D of EPO; the sidechains of both structures are almost identically aligned. Sidechain rotamers of Mutant GCN4 were sampled to find orientations similar to those found in EPO. The residues on the solvent-exposed face of GCN4 fell within the Van der Waals surfaces of residues in Helix D of EPO that are involved in the Site 1 interaction with EPOR (Fig. 18). This suggests that Mutant GCN4 may bind EPOR since its solvent-exposed surface displays a similar binding surface to that of Helix D in EPO. Overlaying the designed coiled coil on EPO shows that Chain B of Mutant GCN4 aligns with Helix D, and Chain A of Mutant GCN4 is oriented in a position closest to Helix B of EPO (Fig. 19). Fig. 20 shows Mutant GCN4 docked beside one EPObp. It represents a theoretical model by which Mutant GCN4 would interact with the EPO receptor. The position of Mutant GCN4 was determined by superimposing it onto EPO complexed with EPObp. To function as an antagonist, the designed coiled coil would likely interact with one receptor through the same seven residues (as mentioned above) that are used by EPO (Fig. 20). This would inhibit the ability of a native EPO molecule to bind two receptor molecules and initiate intracellular signaling events.

Redesigning a small molecule antagonist against EPOR, using a coiled coil scaffold

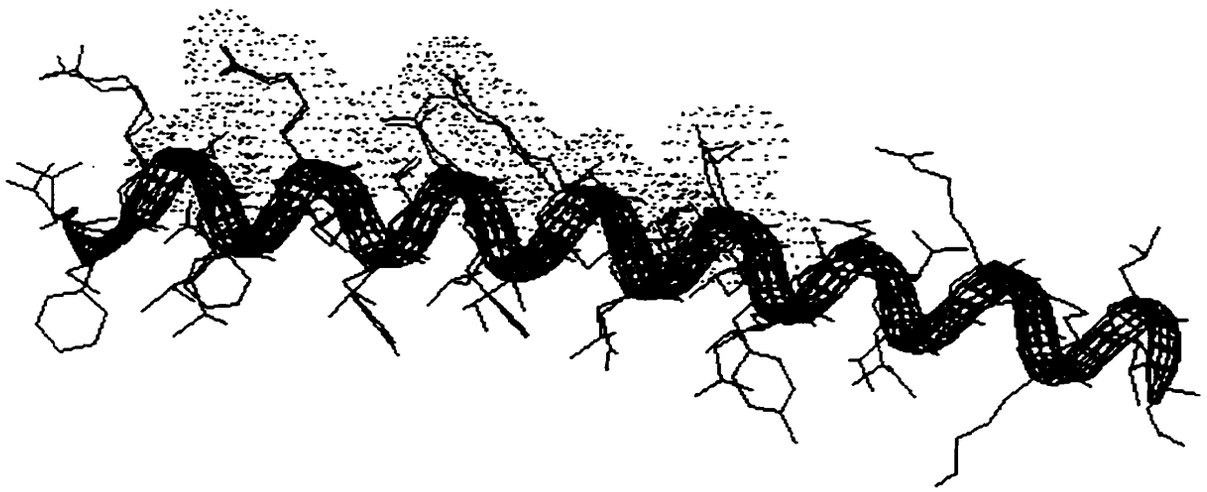

Fig. 18 Chain B of Mutant GCN4 superimposed on Helix D of EPO

Chain B of Mutant GCN4 is shown as a ribbon diagram with backbone and sidechains displayed (blue). Helix D of EPO is shown with backbone and sidechains (red). The Van der Waals surfaces of Lys140, Arg143, Asn147, Arg150, Gly151, Lys154 and Leu155 are shown in red dots. This figure was generated using Swiss-PdbViewer.

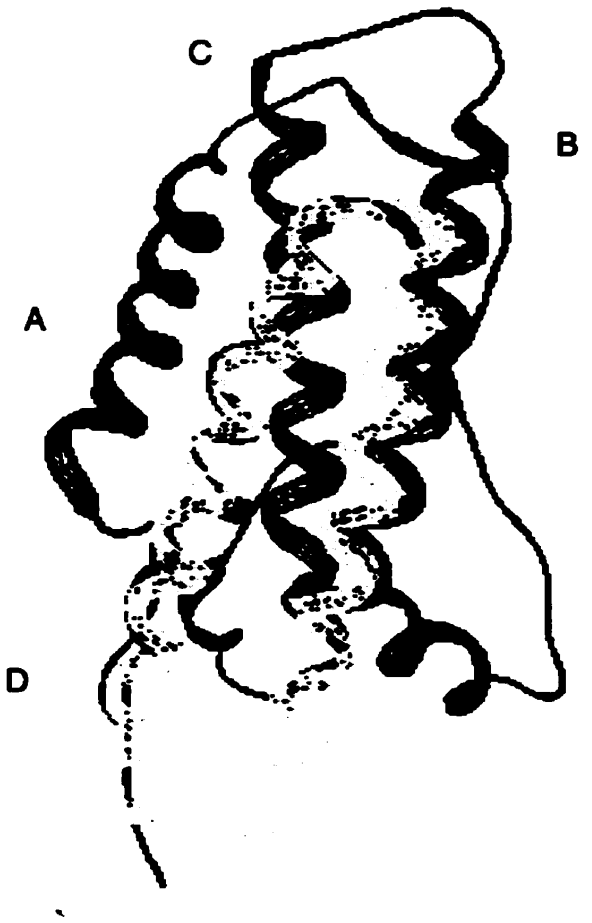

Fig. 19 Superposition of Mutant GCN4 on EPO

Ribbon diagram of Mutant GCN4 (yellow) superimposed on EPO (green). EPO helices are labeled A, B, C and D. One helix (Chain B) of Mutant GCN4 is aligned with Helix D of EPO and the other helix (Chain A) is most closely aligned with Helix B of EPO. This figure was generated using the program Swiss-PdbViewer.

Fig. 20 Mutant GCN4 docked beside EPObp

A ribbon and sidechain representation of the Mutant GCN4 (blue) docked beside one EPObp (red). The seven residues that were transferred from Helix D of EPO, which are biologically important to the Site 1 interaction with EPOR, to Mutant GCN4 are highlighted in green. This diagram was generated using Swiss-PdbViewer.

to present binding residues of EPO, has a high potential for success. Models have shown that the designed EPO antagonist, Mutant GCN4, is able to present the biologically important residues in Helix D, involved in Site 1 binding, to EPOR in a manner similar to EPO. Using the GCN4 leucine zipper motif as a scaffold offers a more native-like structure than the designed 3-helix bundles described in Chapter 2, which were molten globules. The inherent stability of the coiled coil motif may aid in the ability of the designed molecule (Mutant GCN4) to bind EPOR. The GCN4 leucine zipper motif also has the added benefit of presenting a larger EPO binding surface, thus overcoming the potential problem of insufficient binding energy associated with the 3-helix bundle scaffold that was used in the present study. Furthermore, the reduced size of Mutant GCN4, relative to the 3-helix bundles designed in Chapter 2, may minimize any steric hindrance caused by scaffolding helices. In conclusion, using a coiled coil as the helical scaffold to present the binding residues of EPO may be very successful in generating an EPO antagonist.

References

1. Agawa, Y., Lee, S., Ono, S., Aoyagi, H., Ohno, M., Taniguchi, T., Anazai, K., and Kirino, Y. (1991) *J. Biol. Chem.* **266**, 20218-20222

2. Anzai, K., Hamasuna, M., Kadono, H., Lee, S., Aoyagi, H., and Kirino, Y. (1991) *Biochim. Biophys. Acta* **1064**, 256-266

3. Aritomi, M., Kunishima, N., Okamoto, T., Kuroki, R., Ota, Y., and Morikawa, K. (1999) *Nature* **401**, 713-717

4. Barber, D. L., and D'Andrea, A. D. (1994) *Mol. Cell. Biol.* **14**, 6506-6514

5. Barber, D. L., DeMartino, J. C., Showers, M. O., and D'Andrea, A. D. (1994) *Mol. Cell. Biol.* **14**, 2257-2265

6. Barbone, F,. P., Johnson, D. L., Farrell, F. X., Collins, A., Middleton, S. A., McMahon, F. J., Tullai, J., and Jolliffe, L. K. (1999) *Nephrol. Dial. Transplant* **14[Suppl 2]**, 80-84

7. Bazan, J. F. (1990) *Immunol. Today* **11**, 350-354

8. Beck, K., and Brodsky, B. (1998) *J. Struct. Biol.* **122**, 17-29

9. Blondelle, S. E., and Houghten, R. A. (1992) *Biochemistry* **31**, 12688-12694

10. Boissel, J. -P., Lee, W. -R., Presnell, S. R., Cohen, F. E., and Bunn, H. F. (1993) *J. Biol Chem.* **268**, 15983-15993

11. Brandhuber, B. J., Boone, T., Kenney, W. C., and McKay, D. B. (1987) *Science* **238**, 1707-1709

12. Broudy, V. C., Lin, N., Brice, M., Nakamoto, B., and Papayannopoulou, T. (1991) *Blood* **77**, 2583-2590

13. Bryson, J. W., Betz, S. F., Lu, H. S., Suich, D. J., Zhou, H. X., O'Neil, K. T., and DeGrado, W. F. (1995) *Science* **270**, 935-941

14. Butcher, D. J., Kowalska, M. A., Li, S., Luo, Z., Shan, S., Lu, Z., Niewiarowski, S., and Huang, Z. (1997) *FEBS Lett.* **409**, 183-187

15. Chakrabarrty, A., and Baldwin, R. L. (1995) *Adv. Prot. Chem.* **46**, 141-176

16. Chakrabartty, A., Kortemme, T., Padmanabhan, S., and Baldwin, R. L. (1993) *Biochemistry* **32**, 5560-5565

17. Cheetham, J. C., Smith, D. M., Aoki, K. H., Stevenson, J. L., Hoeffel, T. J., Syed, R. S.,

Egrie, J., and Harvey, T. S. (1998) *Nat. Struct. Biol.* **5**, 861-866

18. Cunningham, B. C., and Wells, J. A. (1997) *Current Opinion in Structural Biology* **7**, 457-462

19. D'Andrea, A. D., Lodish, H. F., and Wong, G. G. (1989) *Cell* **57**, 277-285

20. D'Andrea, A. D., Szklut, P. J., Lodish, H. F., and Alderman, E. M. (1990) *Blood* **75**, 874-880

21. D'Andrea, A. D., Yoshimura, A, Youssoufian, H., Zon, L. I., Koo, J. W. and Lodish, H. F. (1991) *Mol. Cel.l Biol.* **11**, 1980-1987

22. Davis, J. M., Arakawa, T., Strickland, T. W., and Yphantis, D. A. (1987) *Biochemistry* **26**, 2633-2638

23. de Vos, A. M., Ultscho, M., Kossiakoff, A. A. (1992) *Science* **255**, 306-312

24. Dexter, T. M., Garland, J., Scott, D., Scolnick, E. M., and Metcalf, D. (1980) *J. Exp. Med.* **152**, 1036-1047

25. Domingues, H., Cregut, D., Sebald, W., Oschkinat, H., and Serrano, L. (1999) *Nat. Struct. Biol.* **6**, 652-656

26. Ebert, B. L., and Bunn, H. F. (1999) *Blood* **94**, 1864-1877

27. Egrie, J. C., Strickland, T. W., Lane, J., Aoki, K., Cohen, A. M., Smalling, R., Trail, G., Lin, F. K., Browne, J. K., and Hines, D. K. (1986) *Immunobiol.* **172**, 213-224

28. Eisenberg, D., Weiss, R. M., and Terwilliger, T. C. (1982) *Nature* **299**, 371-374

29. Eisenberg, D., Weiss, R. M., and Terwilliger, T. C. (1984) *Proc. Natl. Acad. Sci. U. S. A.* **81**, 140-144

30. Elliott, S., Lorenzini, T., Chang, D., Barzilay, J., and Delorme, E. (1997) *Blood* **89**, 493-502

31. Elliott, S., Lorenzini, T., Yanagihara, D., Chang, D., and Elliott, G. (1996) *J. Biol. Chem.* **271**, 24691-24697

32. Epand, R. M., and Scheraga, H. A. (1968) *Biochemistry* **7**, 2864-2872

33. Epand, R. M., Shai, Y., Segrest, J. P., and Anantharamaiah, G. M. (1995) *Biopolmers* **37**, 319-338

34. Erslev, A. (1953) *Blood* **8**, 349-357

35. Fandrey, J. and Bunn, H. F. (1993) *Blood* **81**, 617-623

36. Feng, Y., Klein, B. K., and McWherter, C. A. (1996) *J. Mol. Biol.* **259**, 524-541

37. Foa, P. (1991) *Acta Haematol.* **86**, 162-168

38. Gillis, S., and Smith, K. A. (1977) *Nature* **268**, 154-156

39. Goldberg, M. A., Dunning, S. P., and Bunn, H. F. (1988) *Science* **242**, 1412-1415

40. Grodberg, J., Davis, K. L., and Sytkowski, A. J. (1993) *Eur. J. Biochem.* **218**, 597-601

41. Grodberg, J., Davis, K. L., and Sytkowski, A. J. (1993) *Eur. J. Biochem.* **218**, 597-601

42. Guevara-Aguirre, J., Rosenbloom, A. L., Vaccarello, M. A., Fielder, P. J., de la Vega, A., Diamond, F. B. Jr., and Rosenfeld, R. G. (1991) *Acta Paediatr Scand Suppl* **377**, 96-103

43. Halaby, D., Thoreau, E., Djiane, J., and Mornon, J. P. (1997) *Proteins* **27**, 459-468

44. Harbury, P. B., Zhang, T., Kim, P. S. and Alber, T. (1993) *Science* **262**, 1401-1407

45. Hill, C. P., Anderson, D. H., Wesson, L., DeGrado, W. F., and Eisenberg, D. (1990)

Science **249**, 543-546

46. Ihle, J. N. and Askew, D. (1989) *Int. J. Cell Cloning* **7**, 68-91

47. Itri, L. M. (1992) *Cancer* **70(4 Suppl)**, 940-945

48. Jacobs, K., Shoemaker, C., Rudersdor, R., Neill, S. D., Kaufman, R. J., Mufson, A., Seehra, J., Jones, S. S., Hewick, R., Fritsch, E. F., Kawakita, M., Shimizu, T., and Miyake, T. (1985) *Nature* **313**, 806-810

49. Johnson, D. L., Farrell, F. S., Barbone, F. P., McMahon, F. J., Tullai, J., Kroon, D., Freedy, J., Zivin, R. A., Mulcahy, L. S., and Jolliffe, L. K. (1997) *Chem. Biol.* **4**, 939-950

50. Johnson, D. L., Farrell, F. S., Barbone, F. P., McMahon, F. J., Tullai, J., Hoey, K., Livnah, O., Wrighton, N. C., Middleton, S. A., Loughney, D. A., Stura, E. A., Dower, W. J., Mulcahy, L. S. Wilson, I. A., and Jolliffe, L. K. (1998) *Biochemistry* **37**, 3699-3710

51. Kamtekar, S., Schiffer, J. M., Xiong, H., Babik, J. M., and Hecht M. H. (1993) *Science* **262**, 1680-1685

52. Katsube, T., Fukumaki, Y., Sassa, S., and Miura, Y. (1993) *Blood* **82**, 454-464

53. Klingmüller, U., Bergelson, S., Hsiao, J. G., and Lodish, H. F. (1996) *Proc. Natl. Acad. Sci. USA* **93**, 8324-8328

54. Komatsu, N., Yamamoto, M., Fujita, H., Miwa, A., Hatake, K., Endo, T., Okano, H., Katsube, T., Fukumaki, Y., Sassa, S. and Miura, Y. (1993) *Blood* **82**, 456-464

55. Koury, S. T., Bondurant, M. C., and Koury, M. J. (1988) *Blood* **71**, 524-527

56. Kuwayjima, K. (1989) *Proteins* **6**, 87-103

57. Lacombe, C., and Mayeux, P. (1999) *Nephrol. Dial. Transplant.* **14 [Suppl 2]**, 22-28

58. Lacombe, C., Da Silva, J., Bruneval, P., Fournier, J., Wendling, F., Casadevall, Camilleri, J., Bariety, J., Varet, B., and Tambourin, P. (1988) *J. Clin. Invest.* **81**, 620-623

59. Lansdorp, P. M., Aarden, L. A., Calafat, J., Zeiljemaker, W. P. (1986) *Curr. Top. Microbiol. Immunol.* **132**, 105-13

60. Lin, F. K., Suggs, S., Lin, C. H., Browne, J. K., Smalling, R., Egrie, J. C., Chen, K. K., Fox, G. M., Martin, F., Stabinsky, Z., Badrawi, S. M., Lai, P. H, and Goldwasser, E. (1985) *Proc. Natl. Acad. Sci. USA* **82**, 7580-7584

61. Livnah, O., Johnson, D. L., Stura, E. A., Farrell, F. X., Barbone, F. P., You, Y., Liu, K.

D., Goldsmith, M. A., He, W., Krause, C. D., Pestka, S., Jolliffe, L. K., and Wilson, I. A. (1998) *Nat. Struct. Biol.* **5**, 993-1004

62. Livnah, O., Stura, E. A., Johnson, D. L., Middleton, S. A., Mulcahy, L. S., Wrighton, N. C., Dower, W. J., Jolliffe, L, K., and Wilson, I. A. (1996) *Science* **273**, 464-471

63. Livnah, O., Stura, E. A., Middleton, S. A., Johnson, D. L., Jolliffe, L. K., and Wilson, I. A. (1999) *Science* **283**, 987-990

64. Lupas, A. (1996) *Trends Biochem. Sci* **21**, 375-82.

65. Markowitz, D., Goff, S., Bank, A. (1988) *J. Virol.* **62**, 1120-1124

66. Matthews, D. J., Topping, R. S., Cass, R. T., and Giebel, L. B. (1996) *Proc. Natl. Acad. Sci. U. S. A.* ***93***, 9471-94976

67. McDonald, N. Q., Panayotatos, N., and Hendrickson, W. A. (1995) *EMBO J* **14**, 2689-2699

68. McKnight, C. J., Doering, D. S., Matsudaira, P. T., and Kim, P. S. (1996) *J. Mol. Biol.* **260**, 126-134

69. McMullin, M. F., and Percy, M. J. (1999) *Am. J. Hematol.* **60**, 55-60

70. Middleton, S. A., Barbone, F. P., Johnson, D. L., Thurmond, R. L., You, Y., McMahon, F. J., Jin, R., Livnah, O., Tullai, J., Farrell, F. X., Goldsmith, M. A., Wilson, I. A., and Jolliffe, L. K. (1999) *J. Biol. Chem.* **274**, 14163-14169

71. Milburn, M. V., Hassell, A. M., Lambert, M. H., Jordan, S. R., Proudfoot, A. E., Graber, P., and Wells, T. N. (1993) *Nature* **363**, 172-176

72. Mittl, P. R. E., Deillon, C., Sargent, D., Liu, N., Klauser, S., Thomas, R. M., Gutte, B., and Grütter, M. G. (2000) *Proc. Natl. Acad. Sci. USA* **97**, 2562-2566

73. Miura, O., and Ihle, J. N. (1993) *Arch. Biochem. Biophys.* **306**, 200-208

74. Miyake, T., Kung, C. K.,-H., and Goldwasser, E. (1977) *J. Biol. Chem.* **252**, 5558-5564

75. Muller, T., Oehlenschlager, F., and Buehner, M. (1995) *J. Mol. Biol.* **247**, 360-372

76. O'Shea, E. K., Klemm, J. D., Kim, P. S., and Alber, T. (1991) *Science* **254**, 539-544

77. Palacios, R., and Steinmetz, M. (1985) *Cell* **41**, 727-734

78. Philo, J. S., Aoki, K. H., Arakawa, T., Narhi, L. O., and Wen, J. (1996) *Biochemistry* **35**, 1681-1691

79. Qiu, H., Belanger, A., Yoon, H. -W. P., and Bunn, H. F. (1998) *J. Biol. Chem.* **273**, 11173-11176

80. Qureshi, S. A., Kim, R. M., Konteatis, Z., Biazzo, D. E., Motamedi, H.,. Rodrigues, R., Boice, J. A., Calaycay, J. R., Bednarek, M. A., Griffin, P., Gao, Y. D., Chapman, K., and Mark, D. F. (1999) *Proc. Natl. Acad. Sci. U. S. A.* **96**, 12156-121621

81. Regan, L., and DeGrade, W. F. (1988) *Science* **241**, 976-978

82. Remy, I., Wilson, I. A., and Michnick, S. W. (1999) *Science* **283**, 990-993

83. Robinson, R. C., Grey, L. M., Staunton, D., Vankelecom, H., Vernallis, A. B., Moreau, J. F., Stuart, D. I., Heath, J. K., and Jones, E. Y. (1994) *Cell* **77**, 1101-1116

84. Roehm, N. W., Rodgers, G. H., Hatfield, S. M., and Glasebrook, A. L. (1991) *J. Immunol. Methods* **142**, 257-265

85. Ruscetti, S. K., Janesch, N. J., Chakraborti, A., Sawyer, S. T., and Hankins, W. D. (1990) *J. Virol.* **65**, 1057-1062

86. Schmid, I., Krall, W. J., Uittenbogaart, C. H., Braun, J., and Giorgi, J. V. (1992) *Cytometry* **13**, 204-208

87. Smith, G. P. (1985) *Science* **228**, 1315-1317

88. Somers, W., Stahl, M., and Seehra, J. S. (1997) *EMBO J* **16**, 989-997

89. Syed, R. S., Reid, S. W., Li, C., Cheetham, J. C., Aoki, K. H., Liu, B., Zhan, H., Osslund, T. D., Chirino, A. J., Zhang, J., Finer-Moore, J., Elliott, S., Sitney, K., Katz, B. A., Matthews, D. J., Wendoloski, J. J., Egrie, J., and Stroud, R. M. (1998) *Nature* **395**, 511-516

90. Syed, R. S., Reid, S. W., Li, C., Cheetham, J. C., Aoki, K. H., Liu, B., Zhan, H., Osslund, T. D., Chirino, A. J., Zhang, J., Finer-Moor, J., Elliott, Sitney, K., Katz, B. A., Matthews, D. J., Wendoloski, J. J., Egrie, J., and Stroud, R. M. (1998) *Nature* **395**, 511-516

91. Sytkowski, A. J. and Fisher, J. W. (1985) *J. Biol. Chem.* **260**, 14727-147321

92. Sytkowski, A. J., and Donahue, K. A. (1987) *J. Biol. Chem.* **262**, 1161-1165

93. Taniuchi, H., and Anfinsen, C. B. (1969) *J. Biol. Chem.* **244**, 3864-3875

94. Tian, S. S., Lamb, P., King, A. G., Miller, S. G., Kessler, L., Luengo, J. I., Averill, L., Johnson, R. K., Gleason, J. G., Pelus, L. M., Dillon, S. B., and Rosen, J. (1998) *Science* **281**, 257-259

95. Torti, M., Marti, K. B., Altschuler, D., Yamamoto, K. and Lapetina, E. G. (1992) *J. Biol. Chem.* **267**, 8293-8298

96. Walsh, S. R. R., Cheng, H., Bryson, J. W., Roder, H., and DeGrado, W. F. (1999) *Proc. Natl. Acad. Sci. USA* **96**, 5486-5491

97. Walter, M. R., Cook, W. J., Ealick, S. E., Nagabhushan, T. L., Trotta, P. P., and Bugg, C. E. (1992) *J. Mol. Biol.* **224**, 1075-1085

98. Wang, G. L., and Semenza, G. L. (1993) *Blood* **82**, 3610-3615

99. Watowich, S. W., Hilton, D. J., and Lodish, H. F. (1994) *Mol. Cell. Biol.* **14**, 3535-3549

100. Watowich, S. S., Yoshimura, A., Longmore, G. D., Hilton, D. J., Yoshimura, Y., and Lodish, H. F. (1992) *Proc. Natl. Acad. Sci. USA* **89**, 2140-2144

101. Wells, J. A. (1995) *Biotechnology* **13**, 647-651

102. Wells, J. A. (1996) *Proc. Natl. Acad. Sci. USA* **93**, 1-6

103. Wells, J. A. and de Vos, A. M. (1996) *Annu. Rev. Biochem.* **65**, 609-634

104. Wen, D., Boissel, J. -P., Shower, M., Ruch, B. C., and Bunn, H. F. (1994) *J. Biol. Chem.* **269**, 22839-22846

105. Wilson, I. A., and Jolliffe, L. K. (1999) *Curr. Opin. Struct. Biol.* **9**, 696-704

106. Witthuhn, B. A., Quelle, F. W., Silvennoinen, O., Yi, T., Tang, B., Miura, O., and Ihle, J. N. (1993) *Cell* **74**, 227-236

107. Wlodawer, A., Miller, M., Jaskolski, M., Sathyanarayana, B. K., Baldwin, E., Weber, I. T., Selk, L. M., Clawson, L., Schneider, J., Kent, S. B. (1989) *Science* **245**, 616-621.

108. Wojchowski, D. M., Gregory, R. C., Miller, C. P., Pandit, A. K., and Pircher, T. J. (1999) *Exp. Cell Res.* **253**, 143-156

109. Wrighton, N. C., Balasubramanian, P., Barbone, F. P., Kashyap, A. K., Farrell, F. X., Jolliffe, L. K., Barrett, R. W., and Dower, W. J. (1997) *Nat. Biotechnol.* **15**, 1261-1265

110. Wrighton, N. C., Farrel, F. X., Chang, R., Kashyap, A. K., Barbone, F. P., Mulchahy, L. S., Johnson, D. L., Barrett, R. W., Jolliffe, L. K., and Dower, W. J. (1996) *Science* **273**, 458-463

111. Youssoufian, H., Longmore, G., Neumann, D., Yoshimura, A., and Lodish, H. F. (1993) *Blood* **81**, 2223-2236

112. Zanjani, E. D., Poster, J., Burlington, H., Mann, L. I., and Wasserman, L. R. (1977) *J. Lab. Clin. Med.* **89**, 640-644